6

Interference

Because it is a basic property of every process involving vibrations, interference has been introduced as early as the first chapter of this book. Furthermore, the notion of interference is usually generalized to other domains, quite often far from Physics, such as Economy or Psychology. . . . Two phenomena are said to interfere if their simultaneous actions have new consequences, and if compared with the superposition of the consequences of their independent actions.

General conditions for two light beams to interfere have already been given: they should have exactly, and with high accuracy, the same frequency; their polarizations should not be strictly orthogonal and, last but not least, they must be *coherent with one another*. The fact that two light beams, coming from two independent sources, cannot interfere is rather a good thing, if this were not the case everyday life would occur in a vast field of interference where everything would be striped with interference fringes.

All the experimental set-ups that we are going to describe are supposed to work with incoherent sources. To give the photodetectors the impression that they receive coherent beams, we will always use arrangements in which *all the different interfering beams originate from a unique point source.*

6.1. Wave Front Division Interferometers

The interest of wave front division arrangements is mostly didactic. The prototype of such arrangements was proposed by Young.

6.1.1. *The Young Experiment*

A lamp illuminates, with a light which, for the moment, will be considered as monochromatic (wavelength λ), a tiny hole S with a diameter δ of the order

Chapter 6 has been reviewed by Dr. Dominique Persegol from Schneider Electric.

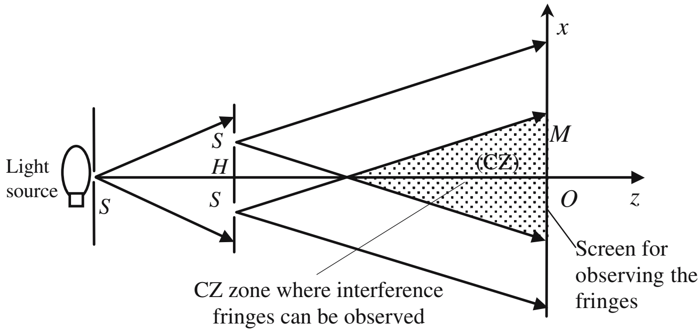

Figure 6.1. Young's experiment. A tiny hole S is illuminated by an extended light source; some light is diffracted inside the first cone inside of which two other holes are placed in close vicinity. S_1 and S_2 can be considered as two coherent sources, interference can be produced in the shadowed area CZ, which is the common zone (CZ) between the two cones of light diffracted from S_1 and S_2. The interference fringes are visible on a screen.

of fifty to hundred times the wavelength. The light wave is diffracted through the hole inside a sharp cone (angle of the order of λ/δ). The light is then diffracted again through the two holes S_1 and S_2 (about the same size as S) which can be considered as two sources emitting the same frequency. If S is at the same distance from S_1 and S_2 the two sources are synchronous, if not, the phase difference is equal to $2\pi(SS_1 - SS_2)/\lambda$. At each point M of the *common zone* (CZ) arrive two beams which have traveled along two different paths SS_1M and SS_2M and have a phase difference equal to $2\pi(SS_1M - SS_2M)/\lambda$. If the difference between the times taken to cover the two paths is smaller than the coherence time of the source S, S_1 and S_2 can be assimilated to coherent sources: interference will then be observable at point M, with maxima if the waves arrive in phase (constructive interference) and minima if they have opposite phases (destructive interference). If the two holes are identical the two sources have the same amplitude and the minima are equal to zero.

To simplify the formulas we consider that $S_1M = S_2M$ and the positions of the maxima and minima are given by

- Maxima: $\psi = \dfrac{2\pi}{\lambda}(MS_2 - MS_1) = (2p+1)\pi \quad \rightarrow \quad (MS_2 - MS_1) = p\lambda.$

- Minima: $\psi = \dfrac{2\pi}{\lambda}(MS_2 - MS_1) = (2p+1)\pi \;\rightarrow\; (MS_2 - MS_1) = (2p+1)\lambda/2.$

The above formulas define a family of revolution hyperboloids; each hyperboloid is labeled by the integer p which is called the *order of interference* along the considered hyperboloid. The intersection of the common zone

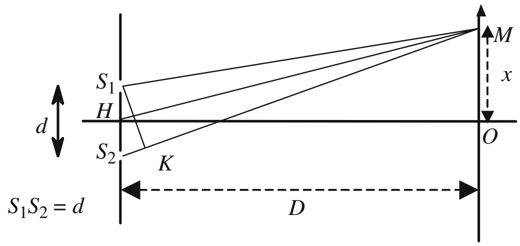

Figure 6.2. Definition of the notations used to describe the Young experiment.

(CZ) and the observation screen seems to be painted with alternately brilliant and dark fringes that are the intersections of a family of hyperboloids with the plane of the screen.

In order to make the fringes brighter, the holes are replaced by narrow parallel slits perpendicular to the plane SS_1S_2. The revolution hyperboloids are then replaced by hyperbolic cylinders, the fringes are parallel to the slits.

To evaluate the state of interference at a given point $M(x)$ we refer to Figure 6.2 in which S_1 and S_2 are two parallel slits. The difference between the phases of the waves arriving at point M corresponds to the propagation of the light from S_2 to K (point of intersection of S_2M with the circle centered at M and of radius MS_1). In all practical situations the distance $d = S_1S_2$ is small in comparison with the distance D to the screen, K can be considered as the projection of S_1 on S_2M:

$$S_2K = x\frac{d}{D}, \quad S_1M = HM - x\frac{d}{2D}, \quad S_2M = HM + x\frac{d}{2D}. \tag{6.1}$$

If S is equidistant from S_1 and S_2, the interferences are *constructive* or *destructive* at points of respective abscissas x_{Max} and x_{min}, given by

$$x_{\text{Max}} = p\frac{\lambda D}{2d} \quad \text{and} \quad x_{\text{min}} = (2p+1)\frac{\lambda D}{2d}, \tag{6.2}$$

$$i = x_{\text{Max}(p+1)} - x_{\text{Max}(p)} = x_{\text{min}(p+1)} - x_{\text{min}(p)} = p\frac{\lambda D}{d}. \tag{6.3}$$

The interference pattern is made of bright and dark bands called interference fringes, they are equidistant and orthogonal to the plane SS_1S_2. The spacing, i, between the centers of two adjacent brilliant, or dark, fringes (see formula (6.3)) is made of the order of a few millimeters by the magnifying ratio D/d; d is a small fraction of one millimeter while D is one meter or more.

We now want the expression of the variation of the light intensity versus abscissa x. We need the expressions of the complex amplitudes of the vibrations at points S_1 and S_2. Of course, we omit the $1/r$ attenuation of the waves and use the expressions $E_1 = \alpha e^{-jkS_1M}$ and $E_2 = \alpha e^{-jkS_2M}$, their superposition gives

$$E_1 + E_1 = \alpha\left(e^{-jkS_1M} + e^{-jkS_2M}\right) = \alpha e^{-jkHM}\left(e^{jk\frac{xd}{2D}} + e^{-jk\frac{xd}{2D}}\right),$$

$$E_1 + E_2 = 2\alpha e^{-jkHM}\cos k\frac{xd}{2D}.$$

The intensity is then given by

$$I = (E_1 + E_2)(E_1 + E_2)^* = 4\alpha^2\cos^2\left(k\frac{xd}{2D}\right), \tag{6.4}$$

$$I = 2\alpha^2\left(1 + \cos k\frac{xd}{D}\right) = 2\alpha^2\left(1 + \cos 2\pi\frac{x}{i}\right). \tag{6.5}$$

6.1.2. *Other Arrangements Using Wave Front Division*

In front of some extended light source is disposed a small hole which, of course, transmits only a small amount of light but which can be considered as a source S of spatially coherent light. The spherical wave diverges and then its wave front is divided into two parts that will follow two different optical paths. In the experimental arrangements that we are going to examine, two optical systems, mirrors and lenses, form two different images of S, these two images play the same role as the Young holes.

The Lloyd mirror arrangements, or some derivative arrangements, are often used for making holographic diffraction gratings. A photoresist is deposited on the mirror. A photoresist is an organic resin made of molecules

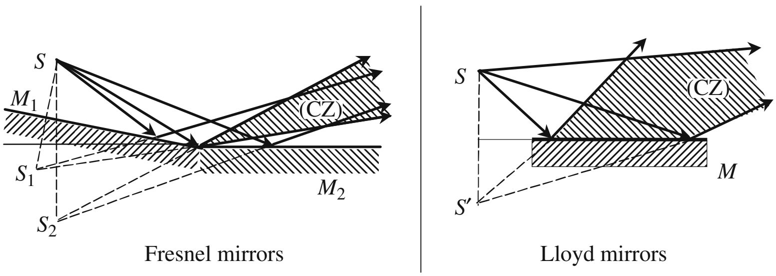

Figure 6.3. Fresnel and Lloyd mirrors. Mirrors are used to duplicate the initial point source S. The point source is in fact replaced by a slit perpendicular to the plane of the figure. Interferences are localized inside the common zone (CZ). In the case of Lloyd mirrors, an extra difference of phase should be added because of the reflection of a dielectric mirror, the zero-order fringe (achromatic) is black.

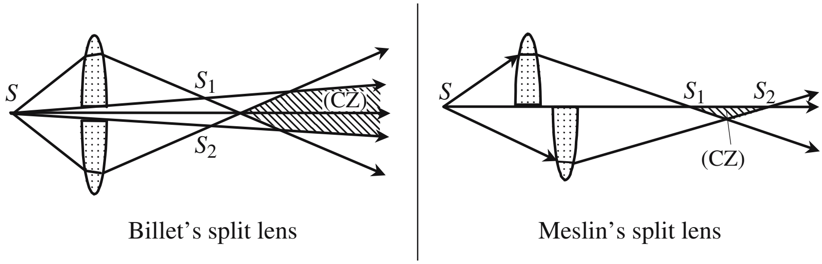

Figure 6.4. Billet's and Meslin's split lenses. A convex lens is sawn along an equatorial plane and the two halves are separated by a small distance, at a right angle to the optic axis for Billet's lenses and along the axis for Meslin's lenses. Two real images are produced from a single point source, S_1S_2 being smaller than the coherence length of S, the two secondary sources can be considered as coherent. In the case of the Meslin arrangement, as one wave passes through a focus, and not the other, the zero-order fringe is dark.

(monomers) that easily polymerize (photopolymerize) if illuminated by a suitable light, giving a solid material. Polymerization is of course more active at the places of brilliant fringes than at the places of dark fringes, after development of the resin the interference pattern has been permanently transferred onto the substrate. The advantage of this arrangement comes from the fact that it is very insensitive to mechanical vibrations, since the light source S and the mirror can be firmly attached together.

6.1.3. *Some Physical Remarks About the Preceding Interference Arrangements*

Two Waves Interference

Along the interference field the law of variation of the light intensity versus position is a sine. Such a law is characteristic of a two-beam interference phenomenon. Let us go back to formulas (6.4) and (6.5), and suppose that one source has been switched off, the light intensity would be constant all over the screen and equal to $I = \alpha^2$, and the energy received per unit of surface proportional to $I = \alpha^2$. When the two beams are sent simultaneously the energy is not constant but spatially modulated as indicated by (6.5), the average value of the energy per unit surface is now $2\alpha^2$, which is consistent with energy conservation: more energy is concentrated in the clear fringes and less in the dark fringes.

Nonlocalized Fringes

Because of the existence of a vast zone (CZ) inside of which interference phenomena may be observed, it is said that the fringes are nonlocalized. Later on we will meet other arrangements where fringes are observable only within restricted areas.

Effect of the Geometric Width of the Slit Sources

To avoid, or at least to limit, the inconvenience of spatial incoherency of the usual light sources, the slits should be as narrow as possible. The slits cannot obviously be completely closed, the question is then: What happens when the slits are progressively enlarged? An exhaustive answer is difficult and needs a description of the electromagnetic boundary conditions at the level of the slit edges. Hopefully the result is not that difficult. On the observation screen the fringes keep their positions, the illumination of dark fringes progressively increases and, at the same time, the clear fringes become less and less brilliant. When the slits become too broad, the screen becomes homogeneously illuminated: the fringes have faded and disappear.

Fringes with Quasi-Monochromatic and White Light, Achromatic Fringe

The wavelength is explicitly written in formulas (6.2) and (6.3) that give the positions of the fringes, which implies that we are using monochromatic beams. At a given point M the two waves coming from points S_1 and S_2 have accumulated a phase difference of geometric origin, the value of which is equal to $2\pi(S_1M - S_2M)/\lambda$. If the arrangement is fully symmetric, it's this phase difference that should be considered for the determination of the state of the interference; if not, some extra phase difference may have to be introduced, this is the case for Lloyd's mirrors (reflection or dielectric mirror) and for Meslin's lenses (passing through a focus), where the phase difference is to be increased of π.

Let us now come back to the symmetrical case, the clear fringes are defined from $(S_1M - S_2M) = p\lambda$, where p is an integer that allows us to label the fringes. The fringe labeled zero, the *zero-order fringe* or the *central fringe*, has the same position whatever the color, this is the reason why it's also designated as the *achromatic fringe*. It is always interesting to see where the achromatic fringe of a given arrangement is; from an experimental point of view the achromatic fringe is easily observed with a white light source, since it is the only noncolored fringe. It's easy to see that for the Lloyd and Meslin arrangements the achromatic fringe is black. The zero-order fringe is the only one to be achromatic, since the spacing between adjacent fringes is proportional to the wavelength.

Far enough away from the achromatic fringe, there is a superposition of the fringes associated with the different colors of the white light: the screen has a white appearance. In fact, some colors are lacking. If the entrance slit of a spectrometer, see Figure 6.6, is at a point where different wavelengths are extinguished, the corresponding colors will not appear and will be

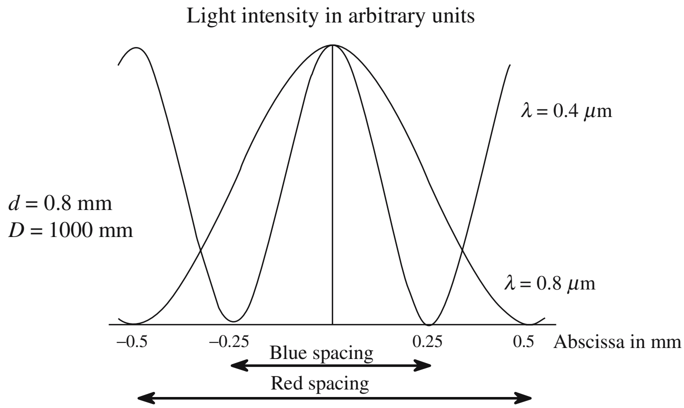

Figure 6.5. Aspect of the achromatic fringe. The red spacing ($\lambda = 0.8\,\mu$m) is twice as broad as the blue spacing ($\lambda = 0.4\,\mu$m). The central part of the fringe which has all the colors is white, the edges seem to be colored in red.

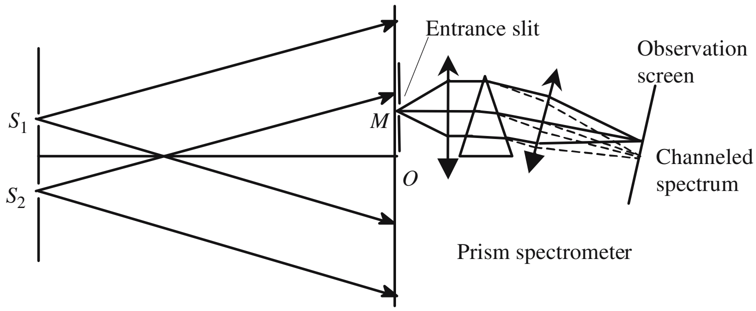

Figure 6.6. Spectral analysis of a channeled spectrum. A spectrometer reveals the presence of brilliant and dark bands parallel to the slits.

replaced by dark bands; the colors with a maximum of intensity will give (brilliant bands. Such a spectrum is called a *channeled spectrum*.

6.2. Amplitude Splitting Interferometers

6.2.1. *Fringes Localization*

Amplitude splitting interferometers are experimental arrangements that allow the observation of interference fringes using extended sources. Of course, a way should be found to alleviate the lack of spatial coherency.

In Figure 6.7 is described the general organization of experimental arrangements of most amplitude splitting interferometers. An incident light

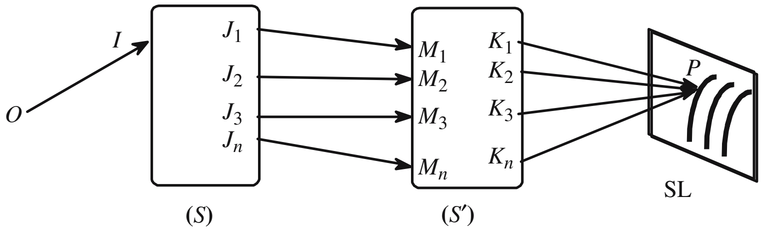

Figure 6.7. Fringe localization. The different rays arriving at P are coherent and may interfere. If a screen has been placed on (SL) it seems that fringes are painted on it.

ray arrives at a first optical system S which generates several different transmitted beams J_1M_1, J_2M_2, $J_3M_3, \ldots, J_nM_n$. A second optical system S' then recombines all these beams to converge toward some point P: *so, to each light ray OI, is associated a point P.* If we now consider a set of incident rays such as OI, we obtain a set of points P, all belonging to a surface SL. On condition that the difference between the times taken by the light in going from O to P are smaller that the coherence time of the source, it can be considered that all the rays arriving at P are coherent and may interfere.

The amplitude of the light vibration at point P is determined by the amplitudes and phases of the vibrations associated to the different rays K_iP. SL is called the surface of localization of the fringes, *it is the only surface along which interferences are observable.* If this surface is real, by opposition to the virtual, it can be covered by an observation screen on which fringes seem to have been painted.

Let $\Phi_1, \Phi_2, \Phi_3, \ldots, \Phi_n$ be the respective phases of the different rays K_iP; very often the arrangement will have been chosen in such a way that the phase difference $\psi = (\Phi_i - \Phi_{I+1})$ is independent of i and is only determined by the initial light ray OI; then at each point P of SL is associated some value of ψ. If $\psi = 2p\pi$ (p is an integer), all the rays arriving at P will interfere constructively: all the points corresponding to the same value of p will be distributed along a curve drawn on SL and called the pth brilliant fringe of interference. In the same way the set of points for which $\psi = (2p + 1)\pi$, ψ will define the pth dark fringe.

Let ξ and η be two coordinates of a point P on the surface SL and let λ be the wavelength, ψ can always be written as a function of ξ and η,

$$\psi = \frac{2\pi}{\lambda} f_{(\xi,\eta)}, \tag{6.6}$$

where $f_{(\xi,\eta)}$ is homogeneous to a length and represents the difference between the optical of two consecutive rays arriving at point P.

It is convenient to classify the interferometers according to the total number n of light rays that are generated by the optical system S, the most interesting cases are:

- $n = 2$, dual beam interferometer.
- $n > 2$, and usually $n >> 2$, multiple beam interferometer.

6.2.2. *Dielectric Films, Double Beam Interference*

A parallel dielectric plate of refractive index n and thickness e is surrounded by a medium of index equal to one, it is illuminated by an extended light source S, wavelength λ. An incident ray SA, because of the numerous reflections on each side of the film, generates two families (R, R', R'', . . .) and (T, T', T'', . . .), interferences are possible, and the localization surfaces are rejected at infinity. The fringes may then be observed in the focal plane of a lens, see Figure 6.9, these are often called *fringes of equal inclination.*

A parallel plate is, a priori, a multiple beam device, however, a simple evaluation of the amplitudes of the successive different reflected beams will show that usually it should be considered only as a dual beam arrangement. The reflection coefficient, at normal incidence, on a dielectric interface is of the order of 4%, under such conditions it's easy to see that the ratios to the initial intensity of ray SA of the respective intensities of the rays R, R', R'', . . . are equal to 4%, 3.8%, and 0.15%: only the first two reflected beams will thus be considered.

Starting from points B and K of Figure 6.8, the two beams R and R' cover equal distances, their phase difference just comes from the difference necessary to travel along ADB which is air and AK which is glass, the optical length difference δ and the phase difference are given by the following expressions, in which i and r are the angles of incidence and of refraction:

$$\delta = n(AD + DB) - AK, \quad \sin i = n \sin r,$$

$$AD = DB = \frac{e}{\cos r}, \quad AB = 2e \tan r, \quad \cos r = \frac{e}{AD},$$

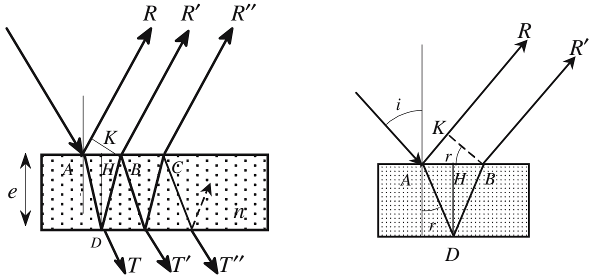

Figure 6.8. The two families of parallel rays generated by reflection on the two sides of a thin film. The localization surfaces are rejected at infinity.

$$AK = AB\sin i = nAB\sin r = 2ne\tan r\sin r = 2ne\frac{\sin^2 r}{\cos r},$$

$$\delta = 2ne\frac{1-\sin^2 r}{\cos r} = 2ne\cos r,$$

$$\delta = 2ne\frac{1-\sin^2 r}{\cos r} = 2ne\cos r + \frac{\lambda}{2} \quad \rightarrow \quad \phi = \frac{2\pi\delta}{\lambda} + \pi = \frac{4\pi ne\cos r}{\lambda} + \pi. \tag{6.7}$$

In equation (6.7) ϕ has been increased by a factor of π, and δ by $\lambda/2$, because of the phase differences occurring at reflection on the two sides of the film.

If δ is equal to an integer number of wavelengths the two reflected beams R and R' interfere constructively, on the contrary they interfere destructively if δ is an odd number of half-wavelengths. Generally speaking, δ is neither odd nor integer, two important parameters are then the *order of interference* p and the *fractional order of interference* ε which are defined as

$$\delta = (p+\varepsilon)\lambda. \tag{6.8}$$

For given values of δ and λ, p is the largest possible integer and ε is smaller than unity. The state of interference is fixed by the fractional order ε.

Nothing very general can be said about the state of interference at normal incidence, the first thing to do is to determine the fractional order of $2ne + \lambda/2$; the order of interference, p, is maximum at normal incidence.

Figure 6.9 shows an experimental set-up that allows the observation of the interference pattern between two waves, respectively, reflected on the two sides of a parallel thin plate at normal, or almost normal, incidence. The light coming from an extended source is sent to the plate using a semitransparent mirror which, on one hand, sends the rays toward the plate and, on the other, from transmits the reflected rays to a lens and then to a screen on which the interference pattern is observed. The fringes are localized in the focal plane of the lens; at each point of this plane two rays arrive, one has been reflected the upper face of the plate and the other the lower face. According to formulas (6.7) and (6.8) their phase difference is the same for all pairs of rays making the same angle with the normal to the plate. The axis of the lens which is orthogonal to the plate is an axis of symmetry: the phase difference and interference state are the same for all rays making the same angle with the axis.

We refer to Figure 6.10, the rays making angle i with the axis are focused at points located at the same distance, fi, from the focal point.

Let $r_1, r_2, \ldots, r_P$ and $i_1, i_2, \ldots, i_P$ be, respectively, the angles of refraction and of incidence for which the phase difference is a multiple of the wavelength: corresponding rays interfere constructively at the point of recombination by the lens where a family of circular clear fringes will be found. Between two adjacent clear rings, there is a dark ring for which the phase difference is an odd multiple of a half-wavelength. P and ε are, respectively, the

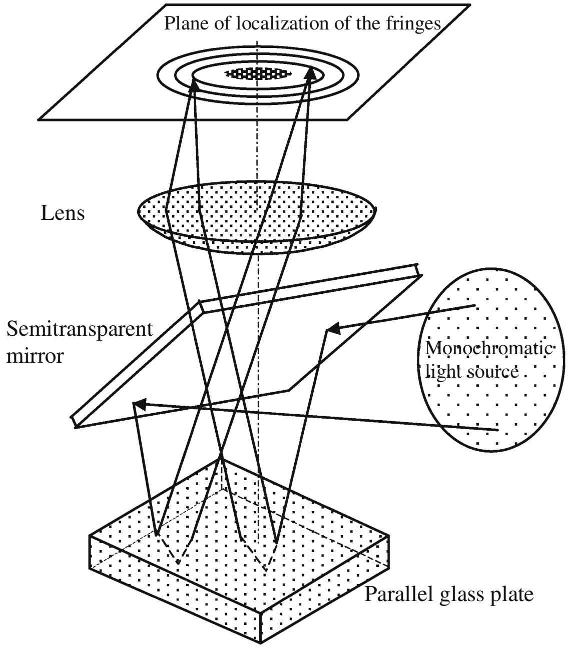

Figure 6.9. Interference after reflection on the two sides of a parallel plate.

order of interference and the fractional excess at normal incidence, the case of clear fringes corresponds to

$$i_1 = nr_1, \quad i_2 = nr_2, \ldots, i_p = nr_p,$$

$$2ne + \frac{\lambda}{2} = (P + \varepsilon)\lambda,$$

$$2ne\cos r_1 + \frac{\lambda}{2} \approx 2ne\left(l - \frac{r_1^2}{2}\right) + \frac{\lambda}{2} = P\lambda,$$

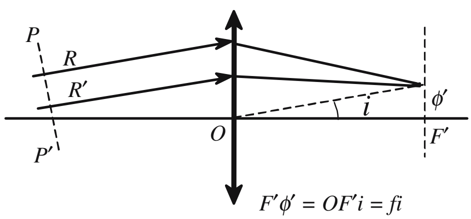

Figure 6.10. Recombination of two parallel rays R and R'. PP'' is the trace of a plane orthogonal to R and R'. After the lens, the transmitted beams intersect at the focal point ϕ'. Because of stigmatism, the two paths $P\phi'$ and $P'\phi$ take the same time: when they arrive at ϕ' the two rays have the same phase difference as in P and P'.

$$2ne\cos r_2 + \frac{\lambda}{2} \approx 2ne\left(1 - \frac{r_2^2}{2}\right) + \frac{\lambda}{2} = (P-1)\lambda,$$

$$2ne\cos r_p + \frac{\lambda}{2} \approx 2ne\left(1 - \frac{r_p^2}{2}\right) + \frac{\lambda}{2} = (P-p+1)\lambda,$$

$$r_p^2 = \frac{(P-1+\varepsilon)\lambda}{ne} \quad \to \quad i_p^2 = n^2 r_p^2 = n\frac{(P-1+\varepsilon)\lambda}{e}.$$

Let us suppose that the fractional excess is just equal to zero at normal incidence, the center of the field pattern is clear. The radii of the different fringes, ρ_1, ρ_2, . . . , ρ_p, are obtained by multiplying the angle of incidence by the focal length and they are proportional to the square roots of the successive integers:

$$\rho_1 = 0, \quad \rho_2 = f\sqrt{\frac{ne}{\lambda}}, \ldots, \rho_P = f\sqrt{\frac{ne}{\lambda}}\sqrt{(P-1)}. \tag{6.9}$$

6.2.3. *Fringes of Slides with a Variable Thickness*

6.2.3.1. *Prismatic Plate*

Interferences given by the prismatic plate of Figure 6.11 can been easily observed by the naked eye of some observer accommodating on the plate, and making the two rays, IR and KR', converge and interfere on the retina. The retina image will be clear at points where the two rays are in phase and dark at points where the phase difference is an odd multiple of π. Finally, the observer gets the impression that the fringes *are painted on the plate.*

The points I, J, and K of Figure 6.11 are very close, $IJ \approx JK$ can be considered as the thickness e of the prism at this point. The difference in the optical length δ of the two rays at point M is the result of two contributions,

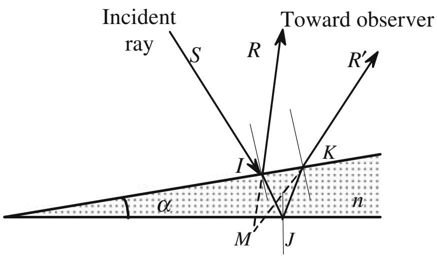

Figure. 6.11. Fringe localization for a prismatic plate. An incident ray SI generates two main reflected rays IR and KR' that are mutually coherent. The determination of the surface of localization is simple only in the case when IR and KR', at some point M that in the case of quasi-normal incidence, remain in close vicinity with the two sides of the prism: the fringes seem to have been painted on the plate.

one has a geometrical origin and the other comes from the difference of the type of reflection of the two beams

$$\delta = 2ne\cos r + \lambda/2 \approx 2ne + \lambda/2.$$

For a clear fringe, the thickness is such that

$$2ne + \frac{\lambda}{2} = p\lambda \quad \to \quad e = \left(p - \frac{1}{2}\right)\frac{\lambda}{2n}.$$

The fringes are lines parallel to the edges of the prism, the difference in thickness $(e_2 - e_1)$ corresponding to two adjacent fringes is obtained by incrementing p of one unit. The fringe separation, i, is constant and is given by

$$(e_2 - e_1) = \frac{\lambda}{2n} \quad \to \quad i = \frac{(e_2 - e_1)}{\tan\alpha} = \frac{\lambda}{2n\tan\alpha} \approx \frac{\lambda}{2n\alpha}. \tag{6.10}$$

6.2.3.2. *Fringes of an Air-Filled Prism*

In the experimental arrangements of Figures 6.12 or 6.8, an incident ray generates several reflected and transmitted beams, we have only drawn those who correspond to air/glass or glass/air reflections. However, four reflected beams still remain; we consider that the thicknesses of the plates are greater than the length of coherence of the light source, which eliminates the interference between the following pairs of rays: RR_1, $R'R'_1$, and $R_1R'_1$. Finally, we only keep the rays R and R': the arrangement becomes equivalent to an air prism which would be limited by two semitransparent mirrors with reflection coefficients of about 4% (intensity). If the wavelength is 0.6 μm and the angle $0.1' = 3 \times 10^{-5}$ rad, formula (6.10) gives a fringe separation of 5 mm.

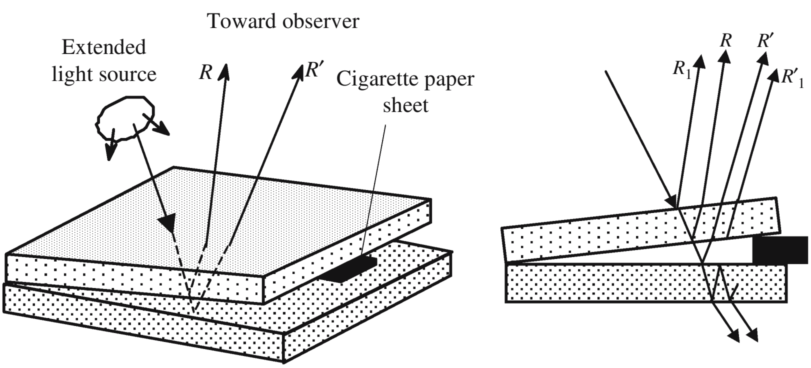

Figure 6.12. Fringes of an air prism. A thin air prism is readily obtained by inserting a thin sheet of paper between the two glass plates.

6.2.3.3. *Fringes of Equal Thickness, Thin Plates Colors*

A prismatic plate, illuminated near its edge, is a special case of a thin transparent medium of nonconstant thickness. It's usual in Physics to use thin dielectric plates, having a good transparency and a thickness of a few micrometers: oil films on a water surface, soap bubbles, faintly oxidized metallic surfaces. . . . Current observation shows that illumination by a white light source produces very pretty interference colors. These colors resemble the wings of some butterflies, the colors of which are also due to interference.

If the film of Figure 6.13 is very thin, the order of interference is not very high and interference fringes may be observed with a white light source. A white source is the superposition of an infinity of monochromatic vibrations, each of which has an infinitesimal amplitude. Let us call $\alpha_\lambda \, d\lambda$ the amplitude of the component of wavelength λ; the different colors cannot interfere and the global intensity, which is the sum of the intensities of the different colors, is proportional to the integral

$$\int_{\text{red}}^{\text{blue}} \alpha_\lambda^2 \, d\lambda = \int_{\text{red}}^{\text{blue}} I_\lambda \, d\lambda, \tag{6.11}$$

where I_λ is a function of the wavelength, the law of variation versus λ determines the special shade of the white light under consideration.

The two rays IR and $I'R'$ of Figure 6.13 that interfere, after having been reflected at a point where the thickness is e, have a difference of optical paths equal to $\delta = 2ne + \lambda/2$; the complex amplitude of the vibration $da_{(\lambda)}$ and the intensity $dI_{(\lambda)}$ are given by

$$da_{(\lambda)} = a_\lambda (1 + e^{-jk(2ne+\lambda/2)}) d\lambda, \tag{6.12.a}$$

$$dI_{(\lambda)} = a_\lambda a_\lambda^* = 4a_\lambda^2 \sin^2\left(\frac{2\pi ne}{\lambda}\right) d\lambda. \tag{6.12.b}$$

If the two reflections are of the same kind it is not necessary to add a phase difference of $\pi/2$ and we then have

$$dI_{(\lambda)} = 4a_\lambda^2 \cos^2\left(\frac{2\pi ne}{\lambda}\right) d\lambda = 4I_\lambda \cos^2\left(\frac{2\pi ne}{\lambda}\right) d\lambda. \tag{6.12.c}$$

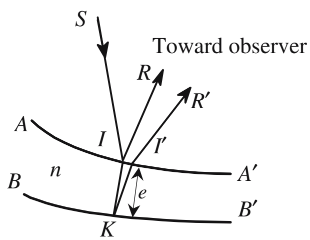

Figure 6.13. The material between the surfaces AA' and BB' is transparent (index of refraction n), its thickness e varies from one point to another. The two rays IR and $I'R'$ combine on the retina of the observer who gets the impression that lines of equal thickness are painted on the film. Dark fringes are obtained when $2ne + \lambda/2 = (2p + 1)/\lambda/2$.

If the plate is thin enough, there will be only a few wavelengths, or eventually only one wavelength, for which the argument of the integrals of (6.11) are equal to zero: illuminated by a white source, the plate takes a color which is characteristic of its thickness. If the thickness is not constant, the fringes of equal thickness are colored. In addition to the aesthetic aspect, this method gives an elegant way to evaluate the thickness of a thin plate; the colors change from straw-yellow to purple as the thickness varies from 280 to 560 nm. The colors obtained by interference of two white light waves is also met on the occasion of the interference between polarized white light beams, and the corresponding calculations are exhaustively developed in Section 5.C.2 of Annex 5.C.

Interference Colors

The colors corresponding to formulas (6.11) and (6.12) are conventionally represented using the following notations:

$$\int I_\lambda \sin^2 \frac{2\pi ne}{\lambda} d\lambda \quad \text{and} \quad \int I_\lambda \cos^2 \frac{2\pi ne}{\lambda} d\lambda,$$

$$\int I_\lambda \sin^2 \frac{2\pi ne}{\lambda} d\lambda + \int I_\lambda \cos^2 \frac{2\pi ne}{\lambda} d\lambda = \int I_\lambda \, d\lambda. \tag{6.13}$$

Formula (6.13) shows that the two different colors, respectively, associated to the same delay δ, are complementary, in the same sense of the word as used by painters. Interference colors are sometimes useful for evaluating, at a glance, the thickness of a thin film. For small delays colorations are bright (as an example, the coloration of butterfly wings are, more or less, the result of an interference process). As the delay is increased the colors get duller to become what is called a *higher-order white*, when the geometric path difference is larger than a few visible wavelengths. The colors that are indicated below are obtained within the two following conditions:

- The spectral composition I_λ of the light source is very similar to the light of the Sun.
- The refractive index dispersion of the film material is negligible; this second condition is fully satisfied in the case of a film of air.

There are many situations in life where interference colors may be observed. Illuminated by a white source, the soap shells of blown bubbles, which have a thickness of a fraction of a micrometer, provide a magnificent illustration of interference colors. In the same way, under white light illumination, the thin films that are obtained when some oil spreads on a wet surface are an illustration of interference colors; because of its nonmiscibility with water, grease tends to have an area as extended as possible and produces extremely thin films, possibly monomolecular. In the case of very small thicknesses, no coloration will appear.

$\delta = ne\ nm$	$\int I_\lambda \sin^2 \frac{2\pi\delta}{\lambda} d\lambda$		$\int I_\lambda \cos^2 \frac{2\pi\delta}{\lambda} d\lambda$	
0	First	black	First	white
40	order	iron gray	order	white
97		lavender gray		yellowish white
158		gray blue		brownish white
218		lighter gray		yellowish brown
234		greenish white		brown
259		white		light red
267		yellowish white		carmine
275		pale straw yellow		dark reddish brown
281		straw yellow	Second	dark violet
306		light yellow	order	indigo
332		bright yellow		blue
430		brown yellow		gray blue
505		reddish orange		bluish green
536		deep red		pale green
551		darker red		yellowish green
565	Second	purple		lighter green
575	order	violet		greenish yellow
589		indigo blue		golden yellow
664		sky blue		orange
728		greenish blue		brownish orange
747		green		light carmine red
826		lighter green		purple
843		yellowish green	Third	purplish
866		greenish yellow	order	violet
910		pure yellow		indigo blue
948		orange		dark blue
998		bright reddish orange		greenish blue
1101		dark purple red		green

6.3. Dual-Beam Interference

6.3.1. *The Michelson Interferometer*

The Michelson interferometer is a very nice optical device, its construction requires the greatest care; the accuracy of the angular and translation position measurements are, respectively, 1 s and 50 nm. One of its most spectac-

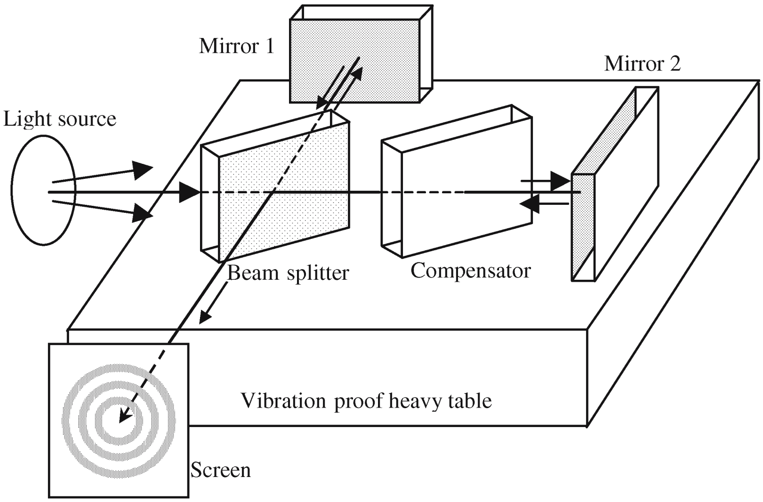

Figure 6.14. The Michelson interferometer.

ular utilizations was made by the physicists Michelson and Morley who gave experimental proof of the fact that the value of the speed of light was independent of the coordinate axis and so brought a demonstration of the validity of Einstein's theory of relativity.

A Michelson interferometer, see Figures 6.14 and 6.15, is made of two mirrors, M_1 and M_2, with high reflection coefficients disposed along two ver-

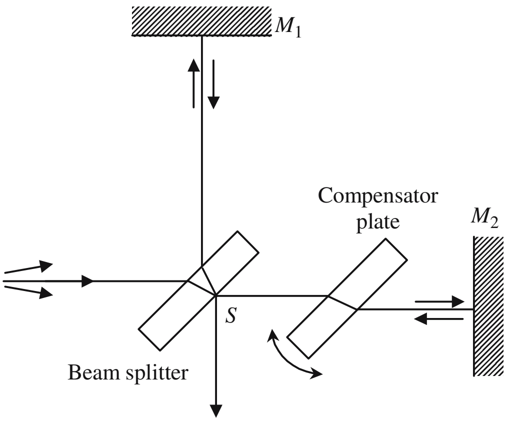

Figure 6.15. Top view of a Michelson interferometer. One interest of this device is to allow the observation of zero- and low-order fringes. M_1 and M_2 can be accurately shifted, the compensator plate is finely rotatable to equalize the length of the two arms SM_1 and SM_2.

tical and orthogonal planes. An important component is the *beam splitter*, another vertical semitransparent mirror making an angle of 45° with M_1 and M_2; one side is antireflection coated, the reflection and transmission coefficients of the other side are equal to 50%. The interferometer is illuminated by an extended monochromatic source. The beam splitter plays two roles: first, it separates the incident beam into two identical beams that are sent to M_1 and M_2 and, second, it recombines them so that they interfere on a screen or a photodetector. The purpose of this interferometer is the observation fringes with a *low order* of interference; the beam that is reflected from mirror M_1 makes an extra double transit inside the beam splitter, this is the reason why a fourth vertical plate, called a compensator plate, is inserted in front of mirror M_2. The compensator plate is almost identical to the beam splitter except that it is antireflection coated on both sides. Rotating finely the compensator plate around a vertical axis allows a fine tuning of the length of SM_1 and makes it equal to SM_2.

A Michelson interferometer has many degrees of freedom, in Figure 6.16 are shown two interesting ways of using it. Let us consider the image M'_2 of the mirror M_2 in the beam splitter, in Figure 6.16(a) M'_2 and M_1 are parallel and separated by a distance e that can be adjusted by a translation of one of the mirrors. The interference pattern is the same as for a parallel plate of the same thickness and filled with air. In Figure 6.16(b), M'_2 and M_1 make a small and adjustable angle, the fringes are those of a wedge plate. If a transparent and weakly inhomogeneous plate P is placed in one arm of the interferome-

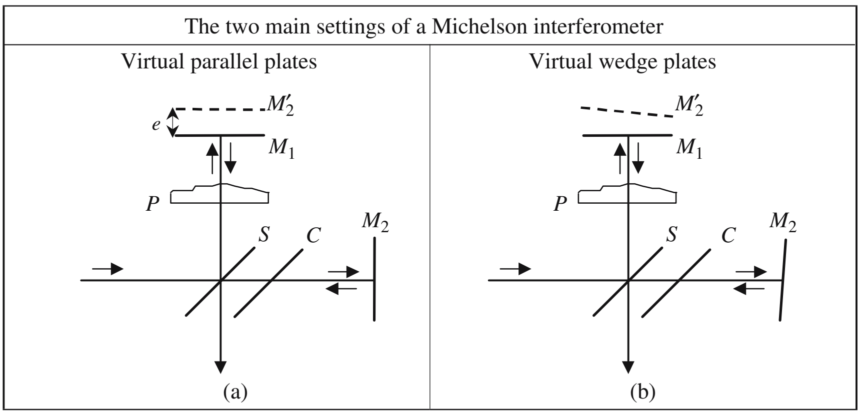

Figure 6.16. M'_2 is the image of M_2 through the beam splitter. According to the adjustment of S, M'_2 and M_1 can be parallel or make a small angle. P is a transparent inhomogeneous plate. In the absence of P, the fringes are concentric rings (virtual parallel plates) or parallel lines (virtual wedge plates). The order of interference being almost zero, the fringes are observable with a white illumination giving typical colored fringes.

ter, the fringe pattern (rings or parallel lines) is modified, and the optical characteristics of the plate are easily obtained from the modifications of the fringes. The method is so sensitive that the variation of the index of refraction of air should be considered.

6.3.2. *The Twyman-Green Interferometer*

The Twyman-Green interferometer is a direct consequence of the Michelson interferometer; its main objective is the characterization of high-quality optical components, such as optical prisms, lenses, or objectives. Disposed in one arm of a Michelson interferometer, the element to be tested is crossed twice by the light rays. In the case of perfect optical quality of the element under test, the return wave and the incident wave are both planar waves, and, according to the setting, usual fringes (parallel plate or wedge plate) are observed. If the optical element has some defects, the return wave is no longer planar, the shape of the fringes is modified, and their modifications give interesting information about the optical imperfections.

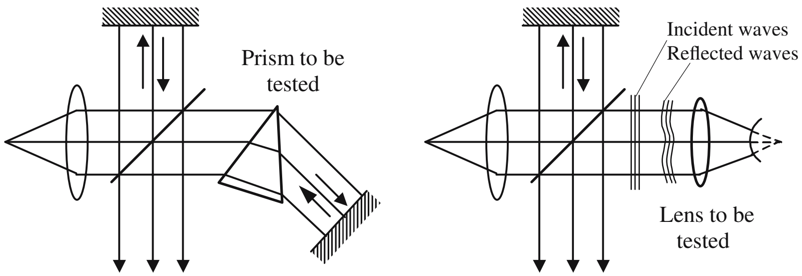

Figure 6.17. Test of optical components using a Twyman-Green interferometer.

6.3.3. *The Mach-Zehnder Interferometer*

The Mach-Zehnder interferometer is described in Figure 6.18; it's a two-wave amplitude splitting interferometer using two beam splitters and two Porro prisms, which can be replaced by two 100% reflecting mirrors. The two arms *ABC* and *ADC* can be given the same optical length and the interference order is almost equal to zero. The two interfering beams travel along two well-separated paths, one is used as a reference (*ADC*), the other (*ABC*) is used for testing some equipment. A Mach-Zehnder interferometer is very convenient for testing refractive index variations occurring inside volumes that can be quite large.

The two emerging beams, *CR* and *CR′*, can be parallel or make a small angle; the fringe pattern is that of a thin parallel plate in the first case, and of a wedge plate in the second case. Before the appearance of laser sources it

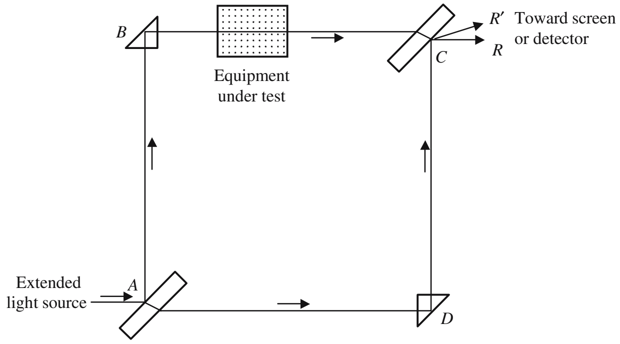

Figure 6.18. Mach-Zehnder interferometer.

was hard work to tune a Mach-Zehnder interferometer; using sources having a long length of coherence considerably simplifies the problem.

In the experimental arrangement of Figure 6.19 the Mach-Zehnder interferometer works as a wedge plate; it is used for characterizing a transparent plate with a step variation of thickness. A lens is used to image the plate on a screen on which the interference fringes of a wedge are superimposed on the image of the plate. Counting the number of fringes allows an accurate measurement of the thickness of the step.

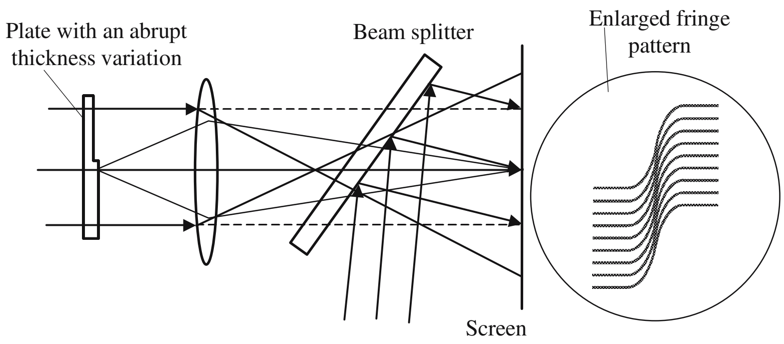

Figure 6.19. Characterization of a thickness variation using a Mach-Zehnder interferometer. Nine fringes may be counted, which corresponds to an optical thickness variation of nine wavelengths.

6.4. The Fabry-Perot Interferometer

It was in an attempt to increase the visibility of the interference fringes that were obtained with thin plates (see Section 6.2.2) that the French physicist Raymond Boullouch, at the end of the nineteenth century, proposed to partially silver the two faces of a glass plate, the purpose being to increase the reflection coefficient and to give it a value higher than 4% which is typical of an air/glass interface. He opened the way to multiple wave interference. Charles Fabry immediately guessed all the spectroscopic possibilities offered by the arrangement of two parallel mirrors and, with the help of Alfred Perot, a very skilled mechanical engineer, gave an experimental demonstration of this fascinating device, which is now universally known as the *Fabry-Perot resonator*, often designated as an FP resonator. The FP resonator is an essential component of most lasers.

6.4.1. *Description of a Fabry-Perot Resonator*

An FP resonator is mainly made of two parallel mirrors, their reflection coefficients are usually high (80–90%) and the parallelism is excellent (10 s $\approx$ 10^{-6} rad).

In Figure 6.20 are shown the two main arrangements of an FP resonator. In Figure 6.20(a) the FP resonator is made of two separate mirrors, each of which is made of a wedge glass plate, one side is coated to have a high reflection coefficient; the two faces are not parallel and make an angle of a few degrees, so that the beams that are reflected on the noncoated faces don't participate in the interference process. A high precision screw allows an accurate translation of the mirrors, which remain parallel while their separation is smoothly varied.

In the arrangement of Figure 6.20(b), reflecting layers are deposited each side of a transparent plate, the faces of which are parallel with a high accuracy. This arrangement, which is known as a *Fabry-Perot etalon*, is very convenient although the separation of the two mirrors is, of course, not tunable.

The performances of an FP resonator come from the quality and the parallelism of the mirrors. The roughness of the faces should be very low, the mean quadratic error with regard to an ideal plane is always better than $\lambda/10$ (λ is some optical wavelength, usually the sodium wavelength) and usually of

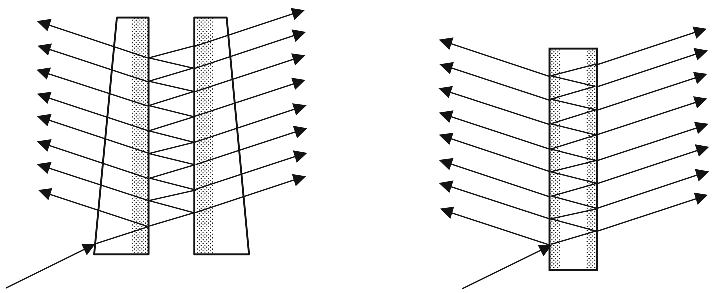

(a) FP Interferometer (b) FP Etalon

Figure 6.20. Examples of an FP resonator.

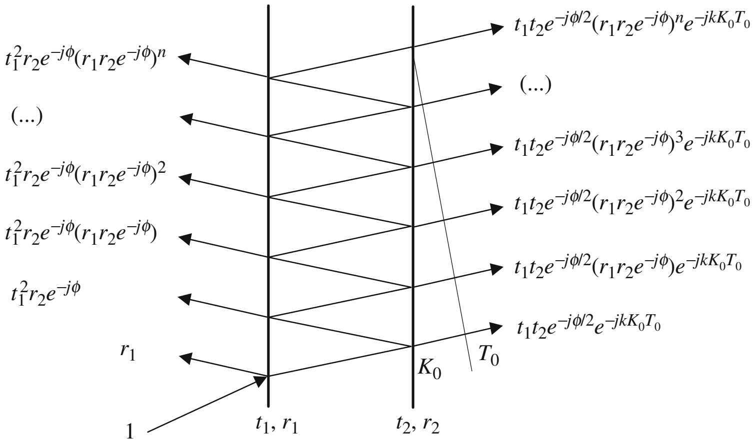

Figure 6.21. Simplified representation of an FP resonator.

$\lambda/100$. Initially, the mirrors were made by metal evaporation, dielectric coatings are now exclusively used, since their absorption coefficients are very low ($0.1\% = 10^{-3}$).

In Figure 6.21 is shown a simplified model that will be used for a theoretical analysis, the glass plates supporting the mirrors are omitted: the resonator is made of two reflective planes separated by a medium having a refractive index equal to one. To each mirror are associated a reflection, a transmission, and an absorption coefficient. Two kinds of coefficients are used corresponding, respectively, to the complex amplitudes or to the intensities of the waves. For complex amplitudes we use lowercase italic letters (r_1, r_2, t_1, t_2, a_1, a_2) and for intensities capital italic letters (R_1, R_2, T_1, T_2, A_1, A_2). The amplitude coefficients are complex numbers, the argument of which is determined by the phase shift occurring at reflection. The intensity coefficients are real and equal to the squared modulus of the amplitude coefficients,

$$R_p = r_p r_p^*, \quad T_p = t_p t_p^*, \quad A_p = a_p a_p^*, \quad R_p + T_p + A_p = 1. \tag{6.14}$$

Referring to Figures 6.21 and 6.22, it is seen that an incident ray generates two families of parallel rays that, respectively, propagate on the left and right sides of the resonator. Since all the rays belonging to a given family are parallel they interfere at infinity and the interference pattern should be observed in the focal plane of a lens L. An FP resonator is usually illuminated by an extended source emitting rays in all directions. To each direction Δ is associated a focus $P(\Delta)$. If the lens is stigmatic, the phase repartition between the different rays is kept on their arrival at $P(\Delta)$ and determines the state of interference. The phase difference between the following two rays is fixed by the angle of incidence i, and remains the same for all the rays making the same angle with the normal to the mirrors. This normal to the mirrors is an axis of

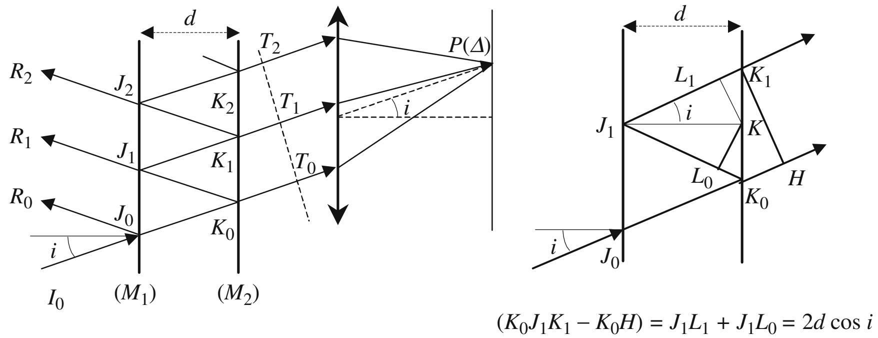

Figure 6.22. Ray trajectories inside an FP resonator. All rays coming from the initial ray I_0J_0 are focused at the same point $P(\Delta)$ where they interfere with the same phases that they had, respectively, at points T_0, T_1, T_2. During the time taken by the ray, which leaves the FP resonator at point K_1 to travel along the optical path $K_0J_1K_1$, the ray leaving at point K_0 will only have covered K_0H.

symmetry, which means that *the interference fringes are concentric circular rings* centered on the focus of the lens corresponding to the direction of the normal.

We must be aware of the fact that the previous treatment is, a priori, not valid since its uses, explicitly and extensively, the notion of light rays to analyze an interference phenomenon, which should be described by waves. The result is however quite correct and there is no paradox at all; the reason is that the resonator is illuminated by planar waves, and a ray like I_0J_0 of Figure 6.22 is just the wave vector of the incident wave, in the same way K_iJ_{i+1} and K_iT_i are the wave vectors of reflected and transmitted waves that are generated on the mirrors.

A planar monochromatic wave (angular frequency $\omega = 2\pi\nu$, vacuum wavelength $\lambda = c/\nu$, vacuum vector $k = 2\pi/\lambda$) illuminates the devices of Figures 6.21 and 6.22, the wave vector is oriented along I_0J_0. The interaction with the first mirror generates a reflected wave J_0R_0 and a transmitted wave J_0K_0, this last wave generates in turn a planar transmitted wave K_0T_0 and a reflected wave K_0J_1, and so on. . . . Almost all analog treatments can be given for the two families of waves, the expressions are slightly simpler for the transmitted waves, because they all follow the same law of recurrence, while the first reflected wave J_0K_0 has a different expression from the others. Although they have equal wave vectors and, consequently, parallel wave planes, all the waves of a given family don't constitute a unique planar wave since there is a phase discrepancy between two successive waves. The phase difference ϕ is evaluated in Figure 6.22:

$$\phi = k2d\cos i = \frac{4\pi d \cos i}{\lambda} = \frac{4\pi d\nu \cos i}{c}. \tag{6.15}$$

6.4.2. *Expressions of the Transmitted Waves, Airy Function*

From the complex amplitudes of the transmitted and reflected waves that are given in Figure 6.21, it is easy to calculate the amplitude $Y(\phi)$ of the wave that is transmitted in the direction which makes an angle i with the normal to the mirrors,

$$Y(\phi) = t_1 t_2 e^{-jkK_0T_0} e^{-j\phi/2} \sum_p \left(r_1 r_2 e^{-j\phi}\right)^p. \tag{6.16}$$

Formula (6.16) is quite general, however, if the reflection coefficients are small the factor $(r_1r_2)^p$ rapidly becomes negligible as p increases. If $r_1 = r_2 = (4\%)^{1/2} \to (r_1r_2)^3 = 6 \times 10^{-5}$, only the two first waves will have some importance in the interference process. Now if $r_1r_2 = 0.8 \to (r_1r_2)^{10} = 0.10$, after ten reflections the signal still has a meaningful value: the FP resonator is really a multiple wave interferometer.

The summation indicated in (6.16) is readily done and the result is

$$Y(\phi) = t_1 t_2 e^{-jkK_0T_0} e^{-j\phi/2} \frac{1}{\left(1 - r_1 r_2 e^{-j\phi}\right)}. \tag{6.17}$$

If the incident wave is given an intensity equal to unity, (6.18) gives the transmitted intensity:

$$I_{t(\phi)} = Y_{(\phi)} Y^*_{(\phi)} = \frac{(t_1t_2)^2}{\left(1 - r_1r_2e^{-j\phi}\right)\left(1 - r_1r_2e^{+j\phi}\right)}, \tag{6.18}$$

$$I_{t(\phi)} = \frac{(t_1t_2)^2}{(1 + r_1r_2)^2 - 2r_1r_2(1 + \cos\phi)} = \frac{(t_1t_2)^2}{(1 + r_1r_2)^2 - 4r_1r_2\cos^2\phi/2}. \tag{6.18.a}$$

We use the reflection ($\rho = r_1r_2$) and transmission ($\tau = t_1t_2$) coefficients for intensities and we define the *coefficient of finesse* F, which is an important parameter of an FP resonator:

$$F = \frac{4\rho}{(1-\rho)^2}, \quad \text{Finesse factor.} \tag{6.19}$$

Using a new function, called the *Airy function*, which is defined by formula (6.20), the intensity is given by formula (6.21):

$$A_{(\phi)} = \frac{1}{1 + F\sin^2\dfrac{\phi}{2}}, \tag{6.20}$$

$$I_{t(\phi)} = \frac{\tau^2}{(1-\rho)^2} A_{(\phi)}. \tag{6.21}$$

According to (6.15), ϕ is proportional to the frequency; the graph $I_{t(\phi)}$ can thus be considered as a representation of the spectral response of the FP resonator.

The Airy function is periodic (2π) and so is the spectral response with a period equal to $2d/c = \tau_{RT}$ (RT for *return time*), τ_{RT} is the time taken by the light to go back and forth between the mirrors. The *finesse factor* such as defined by formula (6.19) is a dimensionless parameter that becomes infinite when the two mirrors are perfectly reflecting. $A(\phi)$ is maximum and equal to one when ϕ is an integer multiple of 2π, and $A(\phi)$ is minimum and equal to $1/(1 + F)$ for odd multiples of π. When F is of the order of unity, or even smaller, the Airy function looks very much like a sine oscillating between 1 and $1/(1 + F)$: it can then be considered that only two beams are interfering. Multiple interferences correspond to high values of the finesse coefficient; as F goes to infinity, $A(\phi)$ becomes a succession of equidistant peaks, with height equal to one and width equal to zero. This is a general property: the higher the number of waves that interfere, the more accurately the condition of positive interference has to be fulfilled; for an infinite number of interfering waves, light is observed only in the directions for which the condition $\phi = p2\pi$ is strictly satisfied.

Finesse and Coefficient of Finesse

Instead of the coefficient of finesse F another parameter is often introduced, it is simply called the *finesse* F_i of the FP resonator and is defined by the following formula:

$$F_i = \frac{\pi}{2}\sqrt{F} = \pi\sqrt{\frac{\rho}{(1-\rho)^2}} = \frac{\pi\sqrt{r_1 r_2}}{(1-r_1 r_2)}, \quad \text{Finesse.} \tag{6.22}$$

Let $\Delta\phi_{1/2}$ be the half-width height of the teeth of the Airy function comb and let ν_p be the frequency of the pth tooth ($\phi = 2p\pi$), for large enough values of the finesse we have

$$\Delta\phi_{1/2} = \frac{4}{\sqrt{F}} \quad \rightarrow \quad F_i = \frac{2\pi}{\Delta\phi_{1/2}}. \tag{6.23}$$

If the graph of Figure 6.23 is considered as the representation of the spectral response of the FP resonator as a function of the frequency ν, the finesse is easily written as a function of the half-width spectral height $\Delta\nu_{1/2}$ on the one hand, and of the frequency difference $(\nu_p - \nu_{p-1})$ between two adjacent teeth on the other hand; this frequency difference $(\nu_p - \nu_{p-1})$ has been given a name: the *free spectral range* (FSR) of the interferometer,

$$F_i = \frac{(\nu_p - \nu_{p-1})}{\Delta\nu_{1/2}}. \tag{6.24}$$

Following a rule of thumb, the finesse is considered to give an order of magnitude for the number of rays that really interfere, since their amplitude is not too small.

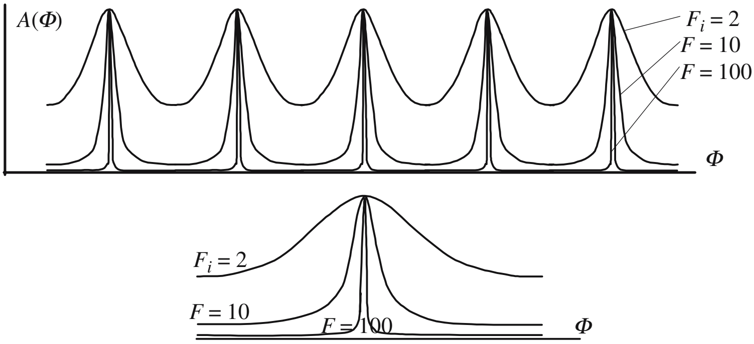

Figure 6.23. Combs of modes for different values of the finesse.

Quality Factor Q

The quality factor Q is a number that is mostly used in electronics to characterize an *RLC* circuit, or the selectivity of a frequency filter; it is defined as the ratio of the central frequency to the bandwidth, it is usually a large number. A Q factor can be defined for the teeth of the comb of mode

$$Q = \frac{\nu_p}{\Delta\nu_{1/2}} = F_i \frac{\nu_p}{(\mathrm{FSR})} = F_i \frac{\nu_p}{(\nu_p - \nu_{p-1})}. \tag{6.25}$$

Numerical Application

We consider an FP resonator with the following optogeometric properties:

$$r_1 = r_2 = 0.96 \quad \rightarrow \quad \rho = 0.92, \quad t_1 = t_2 = 0.282 \quad \rightarrow \quad \tau = 0.08,$$
$$d = 6\,\mathrm{mm}, \quad \tau_{\mathrm{RT}} = 2d/c = 4.10^{-11}, \quad s = 40\ \mathrm{ps}.$$

Ratio of vibrations, respectively, labeled $p = 0$ and $p = 40$ in formula (6.16):

$$\left(\frac{E_p}{E_0}\right)^p = \rho^p = (0.92)^{40} = 0.035 = 3.5\%.$$

Free Spectral Range: (FSR) = $(\nu_p - \nu_{p-1}) = 1/\tau_{\mathrm{RT}} = 2.5 \times 10^{10}$ Hz = 25 GHz.

Finesse factor: $F = \dfrac{4\rho}{(1-\rho)^2} = 575$; Finesse: $F_i = \dfrac{\pi}{2}\sqrt{F} = 37.7 \approx 40.$

Spectral width of a tooth belonging to the comb of modes,

$$\Delta\nu_{1/2} = \frac{(\mathrm{FSR})}{F_i} = 625\ \mathrm{MHz}.$$

Quality factor: $Q = \dfrac{\nu_p}{\Delta\nu_{1/2}} = F_i \dfrac{\nu_p}{(\mathrm{FSR})} = 0.8 \times 10^6.$

The Fabry-Perot Resonator Using Spherical Mirrors

Up to now the waves propagating between the two mirrors were always supposed to be planar and to have an infinite transverse extension, with the nonformulated assumption that the mirrors also have infinite transverse dimensions. . . . If the mirrors don't have an infinite extension, oblique rays, after a great number of reflections, will eventually fall outside the mirrors; this is the reason why the finesse hardly exceeds 50. In the middle of the twentieth century the French physicist Pierre Connes proposed replacing the planar mirrors by spherical mirrors; under such conditions the light rays remain in the vicinity of the line joining the centers of the two mirrors, finesses as high as 1000 can then be reached. Lasers almost exclusively use spherical mirrored resonators.

6.4.3. *Size of the Rings*

We consider the rays that are transmitted through an FP resonator; observed on a screen disposed in the focal plane of a lens, their interference pattern is made of concentric circular fringes, which appear as bright rings on a dark background. Let $FP = x$ be the distance of some point P to the center of the rings and let i be the angle associated to the direction for which P is the focal point. If f is the focal length of the lens, we can write

$$i \approx \tan i = \frac{x}{f} \quad \text{and} \quad \phi = \frac{4\pi d}{\lambda}\cos i.$$

The thickness d of the FP resonator contains a large number of wavelengths, we can always write

$$2d = \lambda(p_0 + \varepsilon), \quad 0 \le \varepsilon \le 1, \quad p_0 \text{ is an integer.} \tag{6.26}$$

ε is a positive number smaller than unity and is called the *fractional excess*.

p_0 is the largest number of half-wavelengths $\lambda/2$, contained in the thickness d, and is called the *order of interference at the center* of the interference pattern.

i being the angle of incidence corresponding to some bright interference ring, we have

$$\sin^2\left(\frac{2\pi d}{\lambda}\cos i\right) = 0 \quad \to \quad \frac{2\pi d}{\lambda}\cos i = p\pi \quad (p \text{ integer}),$$

$$\cos i = \frac{p}{p_0 + \varepsilon}. \tag{6.27}$$

For a given thickness, according to formula (6.27), the order of interference is at most equal to p_0 and decreases with the distance to the center of the interference pattern. For the first clear ring the order of interference is

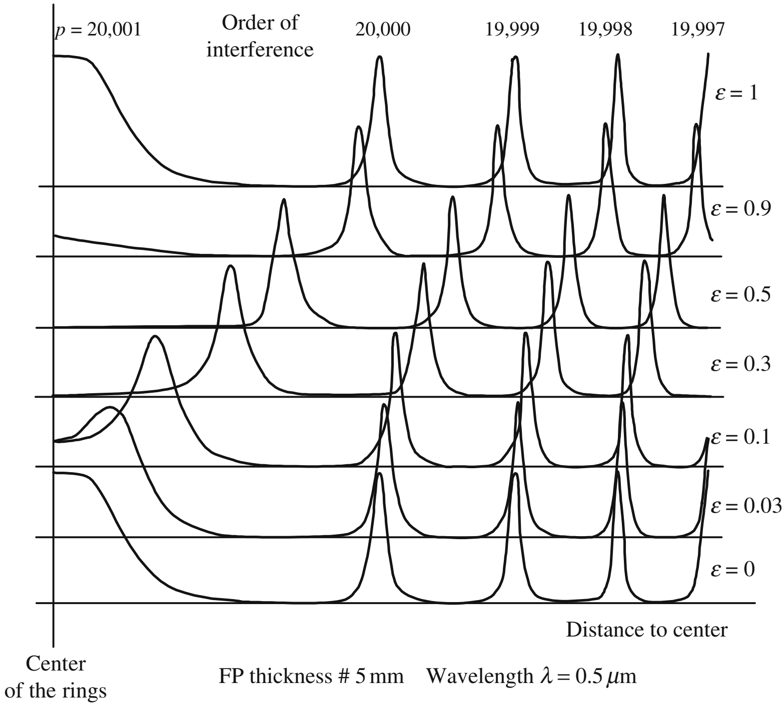

Figure 6.24. Variation of the diameter of the rings as a function of the FP thickness. When the fractional excess $\varepsilon = 0$, we observe a broad and bright spot at the center, surrounded by clear thin rings. As ε increases from 0 to 0.5, a new ring appears, starting from the center.

$p = p_0$, the following rings are obtained by decrementing p, one unit after the other. The angles of incidence of the successive rings are given by the following formulas, in which the angles are considered to be very small:

$$\text{First ring:} \quad \cos i_0 = \frac{p_0}{p_0+\varepsilon} \approx 1 - \frac{\varepsilon}{p_0} \quad \to \quad i_0 \approx \frac{\sqrt{2\varepsilon}}{\sqrt{p_0}}.$$

$$\text{Second ring:} \quad \cos i_1 = \frac{p_0-1}{p_0+\varepsilon} = \frac{p_0}{p_0+\varepsilon} - \frac{1}{p_0+\varepsilon} \approx 1 - \frac{\varepsilon+1}{p_0} \quad \to \quad i_1 \approx \frac{\sqrt{2(\varepsilon+1)}}{\sqrt{p_0}}.$$

$$q\text{th ring:} \quad \cos i_q = \frac{p_0-q}{p_0+\varepsilon} = \frac{p_0}{p_0+\varepsilon} - \frac{q}{p_0+\varepsilon} \approx 1 - \frac{\varepsilon+q}{p_0} \quad \to \quad i_q \approx \frac{\sqrt{2(\varepsilon+q)}}{\sqrt{p_0}}.$$

6.4.4. *Chromatic Resolving Power*

The main purpose of a spectroscope is the examination of the detailed structure of spectral lines; its performances can be described using either the frequency or the wavelength. The chromatic resolution is the smallest wavelength difference $\Delta\lambda_{\min}$, or the smallest frequency difference $\Delta\nu_{\min}$ that can be measured. The chromatic resolving power is the ratio of the wavelength to the chromatic resolution, or of the frequency to the chromatic resolution,

$$R = \frac{\lambda}{\Delta\lambda_{\min}} = \frac{\nu}{\Delta\nu_{\min}}, \tag{6.28}$$

where $\Delta\lambda_{\min}$ is obtained from point C of Figure 6.25(b) and from the expression of the *Airy function* $A(\phi)$ for the two wavelengths λ_1 and λ_2, see formula (6.23),

$$\phi_1 = \frac{4\pi d}{\lambda_1}\cos i = p\pi + \frac{\Delta\phi_{1/2}}{2}, \quad \phi_2 = \frac{4\pi d}{\lambda_2}\cos i = p\pi - \frac{\Delta\phi_{1/2}}{2},$$

$$\frac{4\pi d}{\lambda_1} - \frac{4\pi d}{\lambda_2} \approx \Delta\phi_{1/2} = \frac{2\pi}{F_i} \quad \to \quad 2d\frac{\lambda_2 - \lambda_1}{\lambda_2\lambda_1} \approx \frac{2d}{\lambda}\frac{\Delta\lambda}{\lambda} = p\frac{\Delta\lambda}{\lambda} = \frac{1}{F_i},$$

$$R = \frac{\lambda}{\Delta\lambda} = pF_i. \tag{6.29}$$

The chromatic resolving power is proportional to the coefficient of finesse and to the order of interference.

It is sometimes convenient to introduce the *Free Spectral Range* (FSR) in the expression of $\Delta\lambda_{\min}$:

$$(\mathrm{FSR})_{\text{frequency}} = (\nu_{p+1} - \nu_p) = c\left(\frac{1}{\lambda_{p+1}} - \frac{1}{\lambda_p}\right) \approx c\frac{\lambda_p - \lambda_{p+1}}{\lambda_p^2},$$

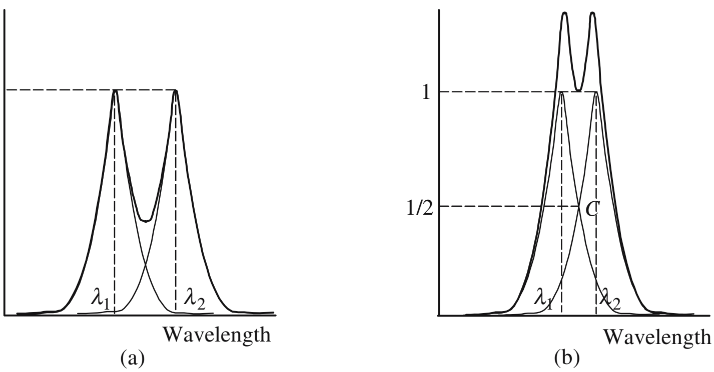

Figure 6.25. Separation of two adjacent rays. Here are shown the intensity profiles of two rings having the same order of interference but two different wavelengths. In (a) the wavelengths are quite different and easily resolved. In (b) the two curves intersect at the point C where the intensity is equal to one-half of the maximum; it is considered that this situation represents the limit of the resolution.

$$(\mathrm{FSR})_{\text{wavelength}} = (\lambda_p - \lambda_{p+1}) \approx \frac{\lambda_p^2}{c}(\mathrm{FSR})_{\text{frequency}},$$

$$\Delta\lambda_{\min} = \frac{(\mathrm{FSR})_{\text{wavelength}}}{F_i}, \quad \Delta\nu_{\min} = \frac{(\mathrm{FSR})_{\text{frequency}}}{F_i}, \tag{6.30}$$

where $\Delta\lambda_{\min}$ is all the smaller as the FP resonator is thicker. Very important thicknesses are not however of practical use, since the different orders of interference would then overlap, making impossible the interpretation of the spectrograms.

Scanning the Fabry-Perot Interferometer

Taking photographs and then performing densitometric measurements has been, for some time, the only way to analyze the interferograms. Direct measurements, using photodetectors, are of course more comfortable; in Figure 6.26 is shown a very convenient arrangement, known as the *Scanning Fabry-Perot* arrangement. As illustrated in Figure 6.24, the diameter of the fringes increases with the distance d between the two mirrors; when d is increased by a half-wavelength, the ring labeled $(q+1)$ takes the place of the ring labeled q. A translation of a fraction of one micrometer is readily obtained with a piezoelectric cell.

The interference pattern is analyzed by a photodetector through a tiny hole, the dimension of which is small as compared to the broadness of an interference fringe. Let us suppose that the light is monochromatic (wavelength λ) and that the hole is located on a clear ring; if the separation between the mirrors is increased, the diameter of the ring also increases: the intensity of the light transmitted through the hole diminishes according to a law which

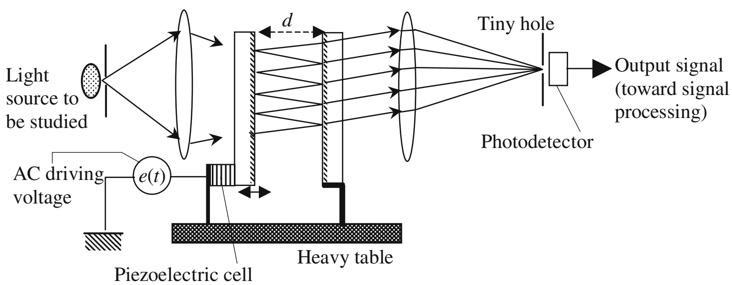

Figure 6.26. Scanning Fabry-Perot arrangement. One of the mirrors is fixed on a piezoelectric cell. The mirror separation, d, is modulated, thanks to a low-frequency (1 kHz) driving voltage $e(t)$. A tiny hole is placed in the focal plane of the second lens in front of a photodetector. The output signal is proportional to the light intensity at the location of the hole.

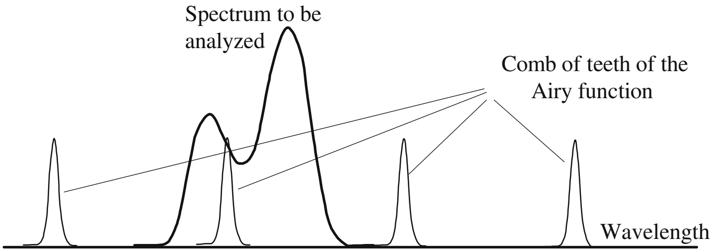

Figure 6.27. Sampling of the spectral profile of a radiation. When the mirror separation d is varied, the frequency distance between two adjacent teeth can be considered to keep a constant value, and the comb is shifted as a whole. The entire Free Spectral Range is swept as d is increased to $\lambda/2$.

is determined by the *Airy function*. We now consider the case of a light source that is no longer monochromatic, that's to say that its intensity is a function, $I(\lambda)$, of the wavelength; however, the variation is supposed to be smooth enough, so that $I(\lambda)$ remains constant inside the frequency band corresponding to the broadness of the ring of the FP resonator: the arrangement of Figure 6.27 allows the sampling of the function $I(\lambda)$ and a suitable signal processing, which takes account of the shape of the *Airy function*, finally giving the profile of I.

6.5. Interference Using Stacks of Thin Transparent Layers

6.5.1. *Considerations About the Technology of Thin Films*

As an answer to the demand in Optics and also in microelectronics, efficient, reproducible, and cheap methods have been developed for depositing thin films on the surface of various substrates. The films can be made of dielectric or metallic materials. Their thicknesses, which range from a few nanometers to a few micrometers, and their chemical composition are controlled with high accuracy. The layers that we will consider here are made of a dielectric material of constant composition and constant refractive index, with a thickness of the order of an optical wavelength (1000 to 10,000 nm).

In most cases, the aim is to elaborate stacks of alternately low-index layers (typically $n = 1.3$) and higher-index layers ($n = 2$), see Figure 6.28. The interesting property of such an arrangement is that its reflection and transmission coefficients vary with the wavelength according to a law that can be easily controlled, by playing on the thickness and on the index of refraction of the layers. A great variety of response curves can be obtained, going from very selective filters to a flat response function inside a given spectral band.

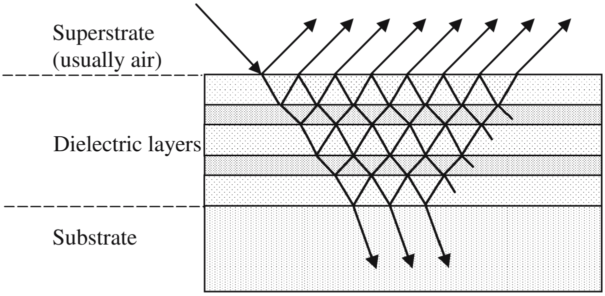

Figure 6.28. Stack of dielectric layers deposited on top of a substrate. An incident wave generates many reflected and transmitted waves. The reflected (or transmitted) wave is the result of the interference of the various partially reflected or transmitted waves.

6.5.2. *Antireflection Coatings*

Antireflection coatings were probably the first industrial applications of thin optical layers. Only one layer is used, its refractive index n_1 is intermediate between the index n_0 of the superstrate and the refractive index n_s of the substrate, see Figure 6.29. The purpose is to obtain that the two first reflected rays, R_1 and R_2, cancel by interference: all the incident energy is then transferred to the transmitted ray. The problem is to determine the index n_1 and the thickness e, so that R_1 and R_2 have the same amplitudes and opposite phases. The incidence is supposed to be quasi-normal, the moduli of the normal reflection coefficient are given by the following expressions:

$$\rho_{\text{superstrate/layer}} = \frac{n_1 - n_0}{n_1 + n_0} \quad \text{and} \quad \rho_{\text{layer/superstrate}} = \frac{n_s - n_1}{n_s + n_1},$$

$$\rho_{\text{layer/substrate}} = \rho_{\text{superstrate/layer}} \quad \rightarrow \quad n_1 = \sqrt{n_0 n_s}\,. \tag{6.31.a}$$

The optical path length difference δ between R_1 and R_2 is equal to

$\delta = 2n_1 e \cos r \approx 2n_1 e,$ since the incidence is normal or almost normal.

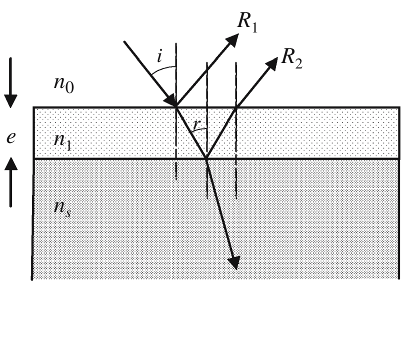

Figure 6.29. Antireflection coating. The incidence is supposed to be quasi-normal. If the index of the layer is equal to $(n_0 n_s)^{1/2}$, and if the thickness is such that a double transit inside the layer produces a phase difference equal to π, then the two reflected rays are mutually destroyed by interference.

The interference will be destructive at the wavelength λ, if the layer thickness is such that $2n_1e = (2p + 1)\lambda/2$, the smallest value of the thickness fulfilling this condition is

$$e = \lambda/4n_1. \qquad (6.31.b)$$

Numerical application: Let us look for a material which would make an antireflection coating, if deposited on a piece of glass suspended in air.

$n_0 = 1$, $n_s = 1 \rightarrow (n_0 n_s)^{1/2} = 1.35$; no convenient material exists with such a low index, the nearest one is cryolithe, AlF_6Na_3, the index of which is 1.35. The deposition of a layer of cryolithe with a suitable thickness on top of a glass slide reduces the normal reflection coefficient from 4% down to 0.3%. All the interfaces of optical instruments, including spectacles, are covered with antireflection coatings. Let us consider the case of a microscope objective made of five different lenses, the light rays will cross ten air/glass interfaces; in the absence of any treatment the ratio of the transmitted intensity to the incident lens is $0.96^{10} = 66\%$, while it becomes $0.997^{10} = 97\%$ with antireflection coatings. The gain of luminosity is not the only advantage; the unwanted reflected light rays constitute a parasitic light signal returning to the eyes of the observer.

If a treated surface is illuminated by a white source, it appears to have a faint blue-violet characteristic color, this comes from the fact that the reflection coefficient is practically equal to zero for a yellow light and has a small, but still appreciable, value for red and blue light rays.

6.5.3. *Generalization to the Case of n Layers*

6.5.3.1. *Matrix Representation of Reflection and Transmission by an Interface*

To determine the waves that are transmitted, or reflected, by an FP resonator, the method used in Section 6.4 consists in the superposition (interference) of the various waves generated on the two mirrors. Although it should be theoretically possible, this method can hardly be generalized to the arrangement shown in Figure 6.28. We are going to follow another way, a matrix will characterize each layer and the action of several cascaded layers will be described using a product of matrices. An excellent description of the matrix treatment of thin layers can be found in the book *Optical Waves in Layered Media* by Pochi Yeh (Wiley).

In Annex 4.A of chapter four it is shown how the invariance in a translation parallel to an interface leads to the conservation of TE and TM polarizations when a beam is reflected or refracted. We refer to Figure 6.30(a and b): the first interface receives a planar wave (wave vector, $\boldsymbol{k}_{1,R}$); a planar reflected wave (wave vector, $\boldsymbol{k}_{1,L}$) and a planar transmitted wave (wave vector, $\boldsymbol{k}_{2,R}$) are created on the first interface. Similarly, a planar reflected wave

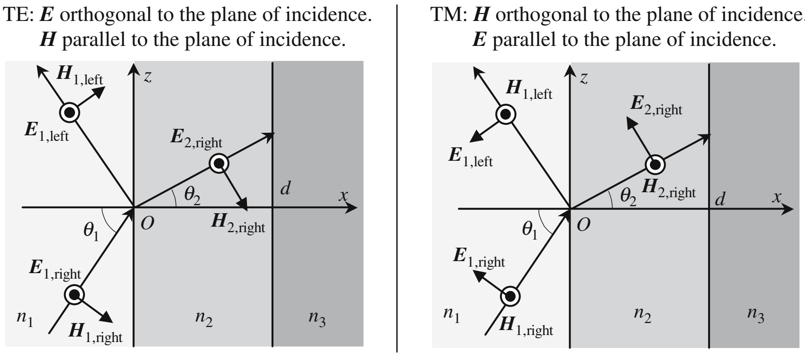

Figure 6.30. TE and TM waves keep their polarization by reflection or refraction.

($\boldsymbol{k}_{2,L}$) and a planar transmitted wave ($\boldsymbol{k}_{3,R}$) are created on the second interface. The labeling conventions are the following:

- 1, 2, 3 refers to the medium inside of which the propagation is made.
- R or L, respectively, mean toward the right- or the left-hand side.

$$\begin{aligned} \boldsymbol{k}_{1,R} &= k_{1,x}\boldsymbol{x} + k_{1,z}\boldsymbol{z}, \quad \boldsymbol{k}_{1,L} = k_{1,x}\boldsymbol{x} + k_{1,z}\boldsymbol{z}, \\ \boldsymbol{k}_{2,R} &= k_{2,x}\boldsymbol{x} + k_{2,z}\boldsymbol{z}, \quad \boldsymbol{k}_{2,L} = k_{2,x}\boldsymbol{x} + k_{2,z}\boldsymbol{z}. \end{aligned} \tag{6.32}$$

If there is only one planar incident wave on the first interface, in the layer labeled α we will find two planar waves with the respective wave vectors $\boldsymbol{k}_{\alpha,R}$ and $\boldsymbol{k}_{\alpha,L}$. These two wave vectors are obtained from the Snell-Descartes laws for refraction and reflection. Because of the orientation chosen for $\boldsymbol{k}_{1,R}$ in Figure 6.30, all the vectors $\boldsymbol{k}_{\alpha,R}$ are parallel to the positive directions of the Ox and Oz axes, while all the $\boldsymbol{k}_{\alpha,L}$ are directed parallel to the positive direction of Ox and the negative direction of Oz. To justify the above allegations, we can either be confident in our physical intuition, other waves being hardly conceivable, or we can say that the solution that we are going to exhibit does satisfy Maxwell's equations, since it's the superposition of planar waves and since it has been specially adjusted to fulfill the boundary conditions along the various interfaces.

According to the Descartes-Snell formula, the projections of all the wave vectors on the axis Oz have the same value β,

$$\begin{aligned} \beta &= k_{1z,R} = k_{1z,L} = k_{2z,R} = k_{2z,L} = k_{3z,R} = k_{3z,L} = \cdots, \\ \beta &= k_1 \sin\theta_1 = k_2 \sin\theta_2 = k_3 \sin\theta_3 = k_\alpha \sin\theta_\alpha = \cdots, \\ \beta &= k_0 n_1 \sin\theta_1 = k_0 n_2 \sin\theta_2 = k_0 n_3 \sin\theta_3 = k_0 n_\alpha \sin\theta_\alpha = \cdots, \end{aligned} \tag{6.33}$$

where $k_0 = \omega/c$ and k_α are, respectively, the moduli of the wave vectors in a vacuum and in a material of refractive n. The projections of the wave vectors on the Ox axis are given by the following formulas:

$$k_{\alpha x,R} = k_0 n_\alpha \cos\theta_\alpha \quad \text{and} \quad k_{\alpha x,L} = -k_0 n_\alpha \cos\theta_\alpha. \tag{6.34}$$

The electric and magnetic fields on both sides of the first interface of Figure 6.30 are given by

$$(\boldsymbol{E}_{1,R}e^{-jk_1x\cos\theta_1}+\boldsymbol{E}_{1,L}e^{+jk_1x\cos\theta_1})e^{j(\omega t-\beta z)} \quad \text{for } x>0, \tag{6.35.a}$$

$$(\boldsymbol{E}_{2,R}e^{-jk_2x\cos\theta_2}+\boldsymbol{E}_{2,L}e^{+jk_2x\cos\theta_2})e^{j(\omega t-\beta z)} \quad \text{for } x>0, \tag{6.35.b}$$

$$\boldsymbol{H}=\frac{j}{\omega\mu_0}\nabla\wedge\boldsymbol{E}. \tag{6.36}$$

For homogeneous and isotropic materials the boundary conditions are very simple: the tangential components of the electric and magnetic fields vary continuously when crossing an interface.

TE Wave

The electric field is along Oy; the magnetic field has two components along Ox and Oz. We set $\boldsymbol{E}_{1,R}=E_{1,R}^{\mathrm{TE}}\boldsymbol{y}$ and $\boldsymbol{E}_{1,L}=E_{1,L}^{\mathrm{TE}}\boldsymbol{y}$ and we obtain

$$\begin{aligned} E_{1,R}^{\mathrm{TE}}+E_{1,L}^{\mathrm{TE}} &= E_{2,R}^{\mathrm{TE}}+E_{2,L}^{\mathrm{TE}}, \\ n_1(E_{1,R}^{\mathrm{TE}}+E_{1,L}^{\mathrm{TE}})\cos\theta_1 &= n_2(E_{2,R}^{\mathrm{TE}}+E_{2,L}^{\mathrm{TE}})\cos\theta_2. \end{aligned} \tag{6.37}$$

If we introduce the matrix

$$\varDelta_\alpha^{\mathrm{TE}}=\begin{pmatrix} 1 & 1 \\ n_\alpha\cos\theta_\alpha & -n_\alpha\cos\theta_\alpha \end{pmatrix}, \quad \alpha\in\{1;2\},$$

equation (6.37) can be written

$$\varDelta_1^{\mathrm{TE}}\begin{pmatrix} E_{1,R}^{\mathrm{TE}} \\ E_{1,L}^{\mathrm{TE}} \end{pmatrix}=\varDelta_2^{\mathrm{TE}}\begin{pmatrix} E_{2,R}^{\mathrm{TE}} \\ E_{2,L}^{\mathrm{TE}} \end{pmatrix}. \tag{6.38}$$

TM Wave

The electric field has two components along Ox and Oz, the magnetic field is along Oyo; we write the continuity of E_z and of H_y:

$$\begin{aligned} (E_{1,R}^{\mathrm{TM}}+E_{1,L}^{\mathrm{TM}})\cos\theta_1 &= (E_{2,R}^{\mathrm{TM}}+E_{2,L}^{\mathrm{TM}})\cos\theta_2, \\ n_1(E_{1,R}^{\mathrm{TM}}-E_{1,L}^{\mathrm{TM}}) &= n_2(E_{2,R}^{\mathrm{TM}}-E_{2,L}^{\mathrm{TM}}), \end{aligned} \tag{6.39}$$

$$\varDelta_\alpha^{\mathrm{TM}}=\begin{pmatrix} \cos\theta_\alpha & \cos\theta_\alpha \\ n_\alpha & -n_\alpha \end{pmatrix} \quad \to \quad \varDelta_1^{\mathrm{TM}}\begin{pmatrix} E_{1,R}^{\mathrm{TM}} \\ E_{1,L}^{\mathrm{TM}} \end{pmatrix}=\varDelta_2^{\mathrm{TM}}\begin{pmatrix} E_{2,R}^{\mathrm{TM}} \\ E_{2,L}^{\mathrm{TM}} \end{pmatrix}, \quad \alpha\in\{1;2\}. \tag{6.40}$$

Fresnel's Formula for Reflection and Refraction

If the second medium is infinitely extended on the positive side of the Ox axis $\to E_{2,L}^{\mathrm{TE}}=E_{2,L}^{\mathrm{TM}}=0$; we can then define the reflection and refraction coefficients: $\rho^{\mathrm{TE}} = (E^{\mathrm{TE}}_{1,L}/E^{\mathrm{TE}}_{1,R})$ and $\tau^{\mathrm{TE}} = (E^{\mathrm{TE}}_{2,R}/E^{\mathrm{TE}}_{1,R})$, and equivalent formulas for the TM waves,

$$\begin{aligned} \rho^{\mathrm{TE}} &= \frac{n_1\cos\theta_1 - n_2\cos\theta_2}{n_1\cos\theta_1 + n_2\cos\theta_2}, \quad \rho^{\mathrm{TM}} = \frac{n_1\cos\theta_2 - n_2\cos\theta_1}{n_1\cos\theta_2 + n_2\cos\theta_1}, \\ \tau^{\mathrm{TE}} &= \frac{2n_1\cos\theta_1}{n_1\cos\theta_1 + n_2\cos\theta_2}, \quad \tau^{\mathrm{TM}} = \frac{2n_2\cos\theta_1}{n_1\cos\theta_2 + n_2\cos\theta_1}. \end{aligned} \tag{6.41}$$

Formulas (6.41) are the same as the Fresnel formulas that have already been established in Section 4.3.3.2, see formulas (4.15) and (4.16).

6.5.3.2. *Representation of a Thin Layer by a* 2×2 *Matrix*

We now come back to the arrangement of Figure 6.30. For a TE polarization there is no discontinuity for the electric vector $\boldsymbol{E}$, since it is purely tangential; the situation is different for the magnetic vector $\boldsymbol{H}$, the normal component of which is discontinuous. For a TM polarization, the magnetic vector is purely tangential and thus continuous, while the normal component of the electric field varies discontinuously.

The full calculation of the matrix method will only be made in the case of a TE polarization. As the electric fields are always parallel, we can forget that they are vectors and treat them as if they were scalar,

$$E_{\alpha(x,z,t)} = \left(E_{\alpha,R}e^{-jk_\alpha x\cos\theta_\alpha} + E_{\alpha,L}e^{+jk_\alpha x\cos\theta_\alpha}\right)e^{j(\omega t-\beta z)},$$

where $E_{\alpha,R}$ and $E_{\alpha,L}$ are constant values inside the layer labeled α; the amplitudes of the waves propagating toward the right- or left-hand side are, respectively, written as:

$$R_{\alpha(x)} = E_{\alpha,R}e^{-jk_\alpha x\cos\theta_\alpha} = E_{\alpha,R}e^{-j(\boldsymbol{k}_\alpha)_x x}, \quad (\boldsymbol{k}_\alpha)_x = k_\alpha\cos\theta_\alpha, \tag{6.42.a}$$

$$L_{\alpha(x)} = E_{\alpha,L}e^{+jk_\alpha x\cos\theta_\alpha} = E_{\alpha,L}e^{+j(\boldsymbol{k}_\alpha)_x x}, \tag{6.42.b}$$

$$x<0 \quad \to \quad (\boldsymbol{k}_\alpha)_x = (\boldsymbol{k}_1)_x = n_1\frac{\omega}{c}\cos\theta_1 = n_1k_0\cos\theta_1,$$

$$0<x<d \quad \to \quad (\boldsymbol{k}_\alpha)_x = (\boldsymbol{k}_2)_x = n_2\frac{\omega}{c}\cos\theta_2 = n_2k_0\cos\theta_2,$$

$$x>d \quad \to \quad (\boldsymbol{k}_\alpha)_x = (\boldsymbol{k}_3)_x = n_3\frac{\omega}{c}\cos\theta_3 = n_3k_0\cos\theta_3.$$

Dropping the label TE, formula (6.38) becomes

$$\varDelta_\alpha = \begin{pmatrix} 1 & 1 \\ n_\alpha\cos\theta_\alpha & n_\alpha\cos\theta_\alpha \end{pmatrix},$$

$$\varDelta_1\begin{pmatrix} R_1(0^-) \\ L_1(0^-) \end{pmatrix} = \varDelta_2\begin{pmatrix} R_2(0^+) \\ L_2(0^+) \end{pmatrix},$$

$$\begin{pmatrix} R_1(0^-) \\ L_1(0^-) \end{pmatrix} = (\varDelta_1)^{-1}\varDelta_2\begin{pmatrix} R_2(0^+) \\ L_2(0^+) \end{pmatrix}, \tag{6.43.a}$$

where 0^- and 0^+ are the abscissas of two points, respectively, located immediately before or immediately after the interface.

The phase difference $\phi_2 = (\boldsymbol{k}_2)_x d$ due to the propagation from the plane $x = 0^+$ to the plane $x = d^-$, and the phase difference $-\phi_2$ for a propagation in the opposite direction, correspond to a propagation matrix P_2,

$$P_2 = \begin{pmatrix} e^{j\phi_2} & 0 \\ 0 & e^{-j\phi_2} \end{pmatrix} \to \begin{pmatrix} R_2(0^+) \\ L_2(0^+) \end{pmatrix} = P_2 \begin{pmatrix} R_2(d^-) \\ L_2(d^-) \end{pmatrix},$$

$$\begin{pmatrix} R_1(0^+) \\ L_1(0^+) \end{pmatrix} = \Delta_1^{-1}\Delta_2 P_2 \begin{pmatrix} R_2(d^-) \\ L_2(d^-) \end{pmatrix} = \Delta_1^{-1}\Delta_2 P_2 \Delta_2^{-1}\Delta_3 \begin{pmatrix} R_3(d^+) \\ L_3(d^+) \end{pmatrix}. \tag{6.43.b}$$

The above formula remains valid for a TM polarization, if the matrix Δ is taken from formula (6.40).

6.5.3.3. *Matrix of an Arrangement of n Layers*

Formula (6.44), which is a generalization of (6.43), is not very convenient for handmade calculations, but proves to be useful if a computer is used,

$$\begin{pmatrix} R_{\text{in}} \\ L_{\text{in}} \end{pmatrix} = \Delta_0^{-1}\left[\prod_1^N \Delta_l P_l \Delta_l^{-1}\right]\Delta_{N+1}\begin{pmatrix} R_{\text{out}} \\ L_{\text{out}} \end{pmatrix},$$
$$\begin{pmatrix} R_{\text{in}} \\ L_{\text{in}} \end{pmatrix} = \begin{pmatrix} M_{11} & M_{12} \\ M_{21} & M_{22} \end{pmatrix}\begin{pmatrix} R_{\text{out}} \\ L_{\text{out}} \end{pmatrix}. \tag{6.44}$$

The matrix elements are obtained from formula (6.34), instead of using the sine or cosine of the angle θ_α, it may be more convenient to use the modulus of the projection on the Ox axis, $k_{\alpha,x} = k_0 n_\alpha \cos\theta_\alpha$, of the wave

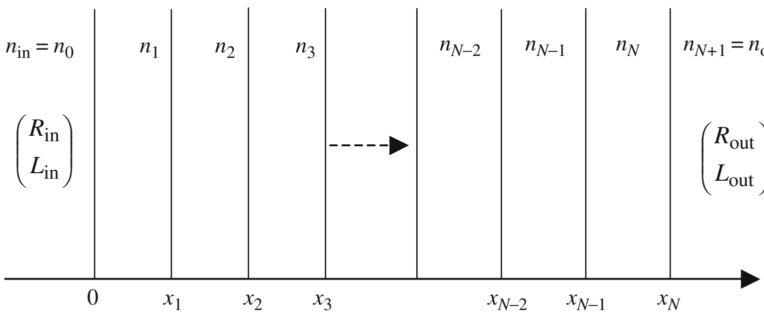

Figure 6.31. Stack of N multidielectric layers sandwiched between a substrate n_{out} and a superstrate n_{in}.

vector

$$\Delta_\alpha^{\mathrm{TE}} = \begin{pmatrix} 1 & 1 \\ n_\alpha \cos\theta_\alpha & -n_\alpha \cos\theta_\alpha \end{pmatrix} = \begin{pmatrix} 1 & 1 \\ k_{\alpha,x}/k_0 & -k_{\alpha,x}/k \end{pmatrix},$$

$$\Delta_\alpha^{\mathrm{TM}} = \begin{pmatrix} \cos\theta_\alpha & \cos\theta_\alpha \\ n_\alpha & -n_\alpha \end{pmatrix} = \begin{pmatrix} k_{\alpha,x}/n_\alpha k_0 & k_{\alpha,x}/n_\alpha k_0 \\ n_\alpha & -n_\alpha \end{pmatrix}.$$

The products of matrices, $D_{l,l+1} = \Delta_l^{-1}\Delta_{l+1}$, that are found in (6.43) and (6.44) have the following expressions:

$$D_{l,l+1}^{\mathrm{TE}} = \begin{pmatrix} \frac{1}{2}\left(1 + \frac{k_{l+1,x}}{k_{l,x}}\right) & \frac{1}{2}\left(1 - \frac{k_{l+1,x}}{k_{l,x}}\right) \\ \frac{1}{2}\left(1 - \frac{k_{l+1,x}}{k_{l,x}}\right) & \frac{1}{2}\left(1 + \frac{k_{l+1,x}}{k_{l,x}}\right) \end{pmatrix}, \tag{6.45.a}$$

$$D_{l,l+1}^{\mathrm{TM}} = \begin{pmatrix} \frac{1}{2}\left(1 + \frac{n_{l+1}^2 k_{l,x}}{n_l^2 k_{l+1,x}}\right) & \frac{1}{2}\left(1 - \frac{n_{l+1}^2 k_{l,x}}{n_l^2 k_{l+1,x}}\right) \\ \frac{1}{2}\left(1 - \frac{n_{l+1}^2 k_{l,x}}{n_l^2 k_{l+1,x}}\right) & \frac{1}{2}\left(1 + \frac{n_{l+1}^2 k_{l,x}}{n_l^2 k_{l+1,x}}\right) \end{pmatrix}. \tag{6.45.b}$$

From a practical point of view, the projection β of the wave vector on the Oz axis will first be evaluated, and then the projection on the Ox axis will be obtained using the following formula (6.46):

$$\beta^2 + k_{\alpha,x}^2 = n_\alpha^2 k_0^2 \quad \rightarrow \quad k_{\alpha,x} = \sqrt{n_\alpha^2 k_0^2 - \beta^2}, \tag{6.46}$$

if $k_{\alpha,x}$ is either real or complex, and if $k_{\alpha,x}$ is real the wave inside the layer of index n_α is a progressive wave. There are two situations for which $k_{\alpha,x}$ is not real: in the first one, the material is absorbing and the index of refraction n_α is a complex number. The second situation is more interesting, the material is fully transparent, n_α is real, but the conditions are those of total internal reflection; $k_{\alpha,x}$ is purely imaginary.

Stack of λ/4 Layers

We now consider the case where the stack of Figure 6.31 is made of the succession of N pairs of layers each having an optical thickness equal to $\lambda/4$ ($n_1 d_1 = n_2 d_2 = n_3 d_3 = \cdots = n_\alpha d_\alpha = \lambda/4$).

According to formulas (6.38) and (6.39), the matrices have the same expression for TE and TM polarizations,

$$\begin{pmatrix} M_{11} & M_{12} \\ M_{21} & M_{22} \end{pmatrix} = \Delta_0^{-1}\left[\Delta_1 P_1 \Delta_1^{-1} \Delta_2 P_2 \Delta_2^{-1}\right]^N \Delta_{2N},$$

$$P_1 = P_2 = \begin{pmatrix} j & 0 \\ 0 & -j \end{pmatrix},$$

$$\begin{pmatrix} M_{11} & M_{12} \\ M_{21} & M_{22} \end{pmatrix} = \Delta_0^{-1}\left[\Delta_1 P_1 \Delta_1^{-1} \Delta_2 P_2 \Delta_2^{-1}\right]^N \Delta_{2N},$$

$$\Delta_1 P_1 \Delta_1^{-1} \Delta_2 P_2 \Delta_2^{-1} = \begin{bmatrix} -n_2/n_1 & 0 \\ 0 & -n_2/n_1 \end{bmatrix}.$$

Finally, we suppose that the last medium is infinitely extended on the positive side of the Ox axis, which means that there is no wave coming back from the right-hand side,

$$L_{2N}(x_{2N}^+) = 0 \quad \rightarrow \quad \begin{pmatrix} R_0(x_0^+) \\ L_0(x_0^+) \end{pmatrix} = \begin{pmatrix} M_{11} & M_{12} \\ M_{21} & M_{22} \end{pmatrix} \begin{pmatrix} R_{2N}(x_{2N}^+) \\ 0 \end{pmatrix},$$

$$R_0(x_0^+) = M_{11} R_{2N}(x_{2N}^+) \quad \text{and} \quad L_0(x_0^+) = M_{21} R_{2N}(x_{2N}^+).$$

We can now evaluate the reflection coefficients of the stack of dielectric layers for either the amplitude or the intensity of the waves,

$$r_{2N} = \frac{L_0(x_0^+)}{R_0(x_0^+)} = \frac{M_{21}}{M_{11}} \quad \text{and} \quad r_{2N} r_{2N}^* = \left|\frac{L_0(x_0^+)}{R_0(x_0^+)}\right|^2 = \left|\frac{M_{21}}{M_{11}}\right|^2,$$

$$r_{2N} r_{2N}^* = \left(\frac{1 - (n_{\text{out}}/n_{\text{in}})(n_1/n_2)^{2N}}{1 + (n_{\text{out}}/n_{\text{in}})(n_1/n_2)^{2N}}\right)^2.$$

$n_0 = n_{\text{in}}$ and $n_{2N+1} = n_{\text{out}}$ are the respective indices of the first and last mediums.

N	0	1	2	3	4	5	6	7
R_{2N}	0.04	0.207	0.425	0.621	0.765	0.860	0.919	0.953
N	8	9	10	11	12	13	14	15
R_{2N}	0.974	0.985	0.992	0.995	0.997	0.998	0.9991	0.9995

The above table gives the values of the reflection coefficient for different values of the number of pairs of layers. The first medium is air ($n_{\text{in}} = 1$), the indices of the two layers of each pair are, respectively, $n_1 = 2$ and $n_2 = 1.4$, the index of the substrate is $n_{\text{out}} = 1.5$.

An important application of dielectric multilayers is the fabrication of mirrors, totally or partly reflecting. The main advantage of using dielectric materials, rather than a metal, is the low value of their absorption coefficients, which is as small as 0.1% (compared with a few per cent for silvered mirrors).

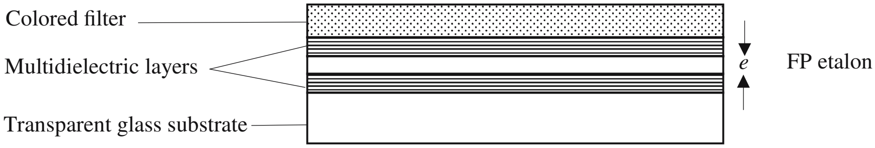

Figure 6.32. Interference filter. The FP etalon only transmits the frequencies of the teeth of the comb of modes. The colored piece of glass is a broader filter centered on the frequency to be selected; it keeps only one tooth and rejects all the others. The substrate is a high-quality piece of glass and ensures mechanical rigidity.

6.5.3.4. *Interference Filter*

An interference filter is used to select a very narrow spectral band of light emitted by a less monochromatic source, they are very common optical components. As shown in Figure 6.32, they are made of an FP etalon, made by depositing dielectric multilayers on both sides of a transparent plate, and of a colored glass plate. The FP etalon transmits all the wavelengths of the different teeth of the comb of modes, its thickness e is adjusted so that one of the teeth just coincides with the frequeqency which is to be selected; if e is small, the frequencies of the adjacent teeth will be quite different and easily removed by a broader band filter.